การพัฒนาเบนซอกซาซีนคอมพอสิทที่เติมแกรไฟต์แกรฟีนท่อนาโนคาร์บอนสำหรับประยุกต์ใช้เป็นแผ่นไบโพลาร์ในเซลล์เชื้อเพลิง

นายสิรวิชญ์ วิทย์ปฐมวงศ์

วิทยานิพนธ์นี้เป็นส่วนหนึ่งของการศึกษาตามหลักสูตรปริญญาวิศวกรรมศาสตรมหาบัณฑิต
สาขาวิชาวิศวกรรมเคมี ภาควิชาวิศวกรรมเคมี
คณะวิศวกรรมศาสตร์ จุฬาลงกรณ์มหาวิทยาลัย
ปีการศึกษา 2560

DEVELOPMENT OF GRAPHITE/GRAPHENE/CARBON NANOTUBES FILLED BENZOXAZINE COMPOSITES FOR BIPOLAR PLATES IN FUEL CELL APPLICATIONS

Mr. Sirawit Witpathomwong

A Thesis Submitted in Partial Fulfillment of the Requirements
for the Degree of Master of Engineering Program in Chemical Engineering
Department of Chemical Engineering
Faculty of Engineering
Chulalongkorn University
Academic Year 2017

Thesis Title	DEVELOPMENT OF GRAPHITE/GRAPHENE/CARBON NANOTUBES FILLED BENZOXAZINE COMPOSITES FOR BIPOLAR PLATES IN FUEL CELL APPLICATIONS
By	Mr. Sirawit Witpathomwong
Field of Study	Chemical Engineering
Thesis Advisor	Professor Sarawut Rimdusit, Ph.D.

Accepted by the Faculty of Engineering, Chulalongkorn University in Partial Fulfillment of the Requirements for the Master's Degree

.....Dean of the Faculty of Engineering

(Associate Professor Supot Teachavorasinskun, D.Eng.)

THESIS COMMITTEE

.....Chairman

(Professor Suttichai Assabumrungrat, Ph.D.)

.....Thesis Advisor

(Professor Sarawut Rimdusit, Ph.D.)

.....Examiner

(Professor Siriporn Damrongsakkul, Ph.D.)

.....External Examiner

(Assistant Professor Chanchira Jubslip, D.Eng.)

สิรวิชญ์ วิทย์ปฐมวงศ์ : การพัฒนาเบนซอกซาซีนคอมพอสิทที่เติมแกรไฟต์แกรฟีนท่อนาโนคาร์บอนสำหรับประยุกต์ใช้เป็นแผ่นไบโพลาร์ในเซลล์เชื้อเพลิง (DEVELOPMENT OF GRAPHITE/GRAPHENE/CARBON NANOTUBES FILLED BENZOXAZINE COMPOSITES FOR BIPOLAR PLATES IN FUEL CELL APPLICATIONS) อ.ที่ปรึกษาวิทยานิพนธ์หลัก: ศ. ดร. ศราวุธ ริมดุสิต, 115 หน้า.

งานวิจัยนี้มีเป้าหมายที่จะพัฒนาแผ่นไบโพลาร์จากพอลิเมอร์คอมพอสิทเพื่อใช้ในเซลล์เชื้อเพลิงชนิดเยื่อแลกเปลี่ยนโปรตอน คุณสมบัติที่สำคัญของแผ่นไบโพลาร์ ได้แก่ ค่าการนำความร้อนสูง ค่าการนำไฟฟ้าสูง ความแข็งแรงและมอดุลัสดัดโค้งสูง และการดูดซึมน้ำต่ำ พอลิเบนซอกซาซีนคอมพอสิทที่เติมหน่วยอนุพันธ์คาร์บอน 3 ชนิด ได้แก่ แกรไฟต์ แกรฟีน และท่อนาโนคาร์บอน ถูกเตรียมด้วยเครื่องอัดขึ้นรูปโดยใช้ความดัน 15 เมกะปาสคาล อุณหภูมิ 200 องศาเซลเซียส เป็นเวลา 2 ชั่วโมง ผลของอัตราส่วนของท่อนาโนคาร์บอนในช่วง 0-2 เปอร์เซ็นต์โดยน้ำหนักแทนที่แกรไฟต์โดยให้อัตราส่วนของแกรฟีนและเบนซอกซาซีนคงที่ที่ 7.5 และ 16 เปอร์เซ็นต์โดยน้ำหนักตามลำดับ ต่อคุณสมบัติของคอมพอสิทถูกนำมาศึกษา การเติมท่อนาโนคาร์บอนลงในคอมพอสิททำให้คุณสมบัติที่สำคัญเพิ่มขึ้น ที่อัตราส่วนท่อนาโนคาร์บอน 2 เปอร์เซ็นต์โดยน้ำหนัก มอดุลัสสะสมที่อุณหภูมิห้องเป็น 11.4 กิกะปาสคาล ขณะที่อุณหภูมิการเปลี่ยนสถานะคล้ายแก้วเป็น 207 องศาเซลเซียส นอกจากนั้นคอมพอสิทจะให้ค่าการนำความร้อนเป็น 21.3 วัตต์ต่อเมตรเคลวิน ให้ค่าการนำไฟฟ้าเป็น 364 ซีเมนต์ต่อเซนติเมตร ให้ค่าความแข็งแรงและมอดุลัสดัดโค้งเป็น 41.5 เมกะปาสคาล และ 49.7 กิกะปาสคาลตามลำดับ จากผลการทดลองแสดงให้เห็นว่าการเติมท่อนาโนคาร์บอนสามารถปรับคุณสมบัติของคอมพอสิทให้เป็นไปตามความต้องการของกรมพลังงานของสหรัฐอเมริกาแสดงว่าเบนซอกซาซีนคอมพอสิทที่เติมแกรไฟต์แกรฟีนและท่อนาโนคาร์บอนเป็นตัวเลือกที่ดีในการประยุกต์ใช้เป็นแผ่นไบโพลาร์ในเซลล์เชื้อเพลิง

ภาควิชา วิศวกรรมเคมี ลายมือชื่อนิสิต .....

สาขาวิชา วิศวกรรมเคมี ลายมือชื่อ อ.ที่ปรึกษาหลัก .....

ปีการศึกษา 2560

5870254721 : MAJOR CHEMICAL ENGINEERING
KEYWORDS: POLYBENZOXAZINE / CARBON NANOTUBES / GRAPHITE / GRAPHENE / BIPOLAR PLATES

SIRAWIT WITPATHOMWONG: DEVELOPMENT OF GRAPHITE/GRAPHENE/CARBON NANOTUBES FILLED BENZOXAZINE COMPOSITES FOR BIPOLAR PLATES IN FUEL CELL APPLICATIONS. ADVISOR: PROF. SARAWUT RIMDUSIT, Ph.D., 115 pp.

This research aims to develop bipolar plate from polymer composite to be used in proton exchange membrane fuel cells. The key properties of bipolar plates include high thermal conductivity, high electrical conductivity, high flexural strength and modulus, and low water absorption. The polybenzoxazine composites having three types of carbon derivatives i.e. graphite, graphene, and carbon nanotubes were prepared using a compression molder with a pressure of 15 MPa and a temperature of 200°C for 2 hours. The effects of carbon nanotube contents varying from 0-2wt% at an expense of graphite with constant content of graphene and benzoxazine at 7.5 and 16wt% respectively on properties of composites were investigated. With an incorporation of carbon nanotubes, relevant properties of the obtained composites increased. At 2wt% carbon nanotubes, storage modulus at room temperature of the samples was 11.4 GPa whereas glass transition temperature was 207°C. Moreover, the composites exhibited thermal conductivity of 21.3 W/m·K, electrical conductivity of 364 S/cm, flexural strength and modulus of 41.5 MPa and 49.7 GPa respectively. Such results indicated that the incorporation of carbon nanotubes could enhanced the properties of the composite to meet those requirement by Department of Energy, USA and confirmed that benzoxazine composites filled with graphite graphene and carbon nanotubes were such a great candidate as bipolar plate in fuel cells application.

Department:	Chemical Engineering	Student's Signature	.....
Field of Study:	Chemical Engineering	Advisor's Signature	.....
Academic Year:	2017		

ACKNOWLEDGEMENTS

The author would like to express my sincerest gratitude and deep appreciation to my advisor, Prof. Dr. Sarawut Rimdusit, for his kindness invaluable supervision, guidance, advice, and encouragement throughout the course of this study. In addition, I would like to thank Prof. Dr. Suttichai Assabumrungrat, Prof. Dr. Siriporn Damrongsakkul, and Asst. Prof. Dr. Chanchira Jubsilp for their invaluable comments as thesis committees.

This research has financial support from the Ratchadapisek Sompoch Endowment Fund, Chulalongkorn University (CU-59-029-AM) and the Institutional Research Grant Chulalongkorn University Contract (No. RES_57_ 411_21_076).

I would like to thanks Toyo Tanso (Thailand) Company Limited for the kind support of graphite. Thanks to Department of Materials Science, Faculty of Science, Chulalongkorn University for the support in the use of ball mill to crush graphite and Mektec Manufacturing Corporation (Thailand) Limited for the support in the use of laser flash apparatus.

In addition, I would like to thanks all members of Polymer Engineering Laboratory, Department of Chemical Engineering, Faculty of Engineering, Chulalongkorn University for their guidance, assistance, discussion, and sincerely encouragement in solving problems. Finally, my deepest regards to my family members who have always been the source of my unconditional love, understanding, and generous encouragement during my studies. Also every person who deserves thanks for encouragement and support that cannot listed.

CONTENTS

Page

Page

Page

Page

LIST OF TABLES

Page

LIST OF FIGURES

CHAPTER I

INTRODUCTION

1.1 General Introduction

Fuel cell is a device which provides energy from chemical reaction or redox reaction [1-4]. It is used as an energy source along with battery but fuel cell can generate energy continuously if fuels are still supplied. Hydrogen and oxygen are two types of fuels used in fuel cell. Water is only a product generated from fuel cell so there is no pollution problem.

Figure 1.1 Fuel cells [5].

Nowadays, proton exchange membrane fuel cells (PEMFCs) is known as the most popular types of fuel cells used as an alternative source of energy because of providing high power density, long lifetime, low cost, releasing non-toxic substance and low operating temperature (50-80 ^{o}C) [3].

Bipolar plates are one of the important components of PEMFCs because their weight is about 60-80% and costs 40-50% of the whole cells [6-8]. They have many functions such as withstand external force, separate unit cell of other cells in stack, manage hydrogen, oxygen, heat, current and water inside the cell [4, 8-11]. To achieve all of these functions completely, bipolar plates must have good thermal, mechanical, electrical and chemical properties which required by Department of energy, USA (DOE). The bipolar plates used for PEMFCs must have electrical conductivity > 100 S/cm, thermal conductivity > 20 W/m·K, flexural strength > 25MPa, water absorption at 24 h < 0.3% [11-14]. Moreover, they must provide light weight and low cost.

To achieve all properties required by DOE, polymer composites were developed to apply as bipolar plates. Polymers as resin binder are classified into two types i.e. thermoplastic and thermosetting. Thermosetting polymer is more usability than thermoplastic because its low melt viscosity facilitates easy fabrication of the composite. Polybenzoxazines are new types of thermosetting polymer which possess low melt viscosity, high thermal stability, low water absorption, good mechanical strength and no by-product generated from their curing process [15-20]. Morever, large

amount of filler can be filled in the polybenzoxazine matrix by take advantage of low melt viscosity.

Graphite has gain much attention from many researchers for developing high conductivity composite material. It was filled in the polymers to increase thermal conductivity, electrical conductivity, flexural strength, and flexural modulus and also decrease water absorption. I. Dueramae *et al.* [21], S.R. Dhakate *et al.* [22] and Kimura *et al.* [23] were achieved to fill graphite into polymer composites and provide outstanding properties.

Recently, new derivatives of carbon such as carbon nanotubes and graphene were discovered. They have high intrinsic thermal and electrical conductivity, high aspect ratio, low density and good mechanical properties [8]. They became a good selective to use as fillers in the composites. R. Plengudomkit *et al.* [7] were accomplished to develop highly-filled graphene polymer composites with better properties than that of highly-filled graphite polymer composites.

Moreover, hybrid fillers polymer composites were accomplished and provided advantages of each filler. A number of researches showed that fillers will have synergistic effect each other if composites have optimal ratio of each filler. The composites with hybrid fillers have better properties than composites with only type of filler [24-28]. However, thermal conductivities of the composites were lower than DOE target. S.R.Dhakate *et al.* [25] developed composite filled with graphite and carbon nanotubes in which thermal conductivity was enhanced to 13 W/m·K while

M.Phuangngamphan [29] developed polybenzoxazine composite filled with graphite and graphene to provide thermal conductivity of the composite up to 14.5 W/m·K. From these researches, graphite, graphene, and carbon nanotubes were selected as conductive fillers filled in polybenzoxazine matrix to develop bipolar plates with higher thermal conductivity.

This research aims to develop polybenzoxazine composite filled with three fillers: graphite, graphene and carbon nanotubes and study effects of carbon nanotubes on physical, mechanical, thermal and electrical properties of the composite.

1.2 Objectives

1.2.1 To determine maximum packing density of benzoxazine composites filled with graphite.

1.2.2 To evaluate effects of multi-wall carbon nanotube contents on thermal, electrical and mechanical properties of benzoxazine composite filled with graphite and graphene.

1.3 Scopes of the study

1.3.1 Synthesis of benzoxazine resin by solventless technology.

1.3.2 Determination of the optimum composition of graphite-filled benzoxazine by varying compositions of graphite at 70wt%, 75wt%, 80wt%, ..., maximum packing density.

1.3.3 Fixing composition of graphene at 7.5wt% and varying composition of multi-walled carbon nanotubes from 0-2wt% at an expense of graphite and evaluation properties of graphite/graphene/multi-wall carbon nanotubes benzoxazine composite by

1.3.3.1 Dynamic mechanical analyzer (DMA)

1.3.3.2 Thermogravimetric analyzer (TGA)

1.3.3.3 Differential scanning calorimeter (DSC)

1.3.3.4 Laser flash diffusivity

1.3.3.5 Universal testing machine (UTM)

1.3.3.6 Water absorption measurement

1.3.3.7 Electrical conductivity measurement (four point probe method)

1.3.3.8 Density accessory kit

1.3.3.9 Scanning electron microscope (SEM)

1.4 Procedure of the study

1.4.1 Reviewing related literature.

1.4.2 Preparation of chemicals and equipment to be used in this research such as bisphenol A, paraformaldehyde, aniline, graphite, graphene, and multi-walled carbon nanotubes.

1.4.3 Synthesis of benzoxazine resins (BA-a) by solventless technique.

1.4.4 Preparation of graphite-filled benzoxazine composites by varying graphite contents at 70 wt%, 75 wt%, 80 wt%,..., maximum packing density.

1.4.5 Preparation of graphite/ graphene/ multi- walled carbon nanotubes benzoxazine composites by fixing graphene contents at 7.5 wt% and varying graphite and multi-walled carbon nanotubes contents.

1.4.6 Determine properties of the composites as follow:

1.4.6.1 Physical properties: density, water absorption, and fracture surface

1.4.6.2 Thermal properties: glass transition temperature, degradation temperature, specific heat capacity, thermal diffusivity, and thermal conductivity

1.4.6.3 Electrical properties: electrical conductivity

1.4.6.4 Mechanical properties: flexural strength and flexural modulus

1.4.7 Analysis of the experimental results.

1.4.8 Preparation of the final report.

CHAPTER II

THEORY

2.1 Fuel Cell

Fuel Cell is an instrument which provides energy from electrochemical reactions [2-4]. The reactions named oxidation and reduction reaction occured in electrodes called anode and cathode respectively and there is a layer called electrolyte located between two electrodes.

Fuel cells are classified based on type of electrolyte into five main types: alkaline fuel cells (AFCs), phosphoric acid fuel cells (PAFCs), proton exchange membrane fuel cells or polymer electrolyte membrane fuel cells (PEMFCs), molten carbonate fuel cells (MCFCs) and solid oxide fuel cells (SOFCs) [2].

Alkaline fuel cells (AFCs) are consisted of matrix which adsorbing concentrated KOH solution. They are used in space shuttle program. They have high rate of cathodic reaction but suffer contamination problems.

Phosphoric acid fuel cells (PAFCs) are composed of polytetrafluoroethylene-bonded silicon carbide as a matrix and concentrated phosphoric acid as an electrolyte. They are able to resist corrosion and contamination and provide high power.

Proton exchange membrane fuel cells or polymeric electrolyte membrane fuel cells (PEMFCs) are consisted of polymeric electrolyte such as sulfonated polyether ether ketones (SPEEK) or polybenzimidazoles (PBI).

Molten carbonate fuel cells (MCFCs) are based on ceramic matrix of $LiAlO_2$ and alkali carbonates as solid electrolyte. They can be operated in high temperature environment (600-800 ^{o}C). Catalyst is unessential to use for these fuel cells.

Solid oxide fuel cells (SOFCs) are composed of ZrO_2 stabilized with Y_2O_3 as electrolyte. Similar to MCFCs, they resist high temperature (600-1,000 ^{o}C) and catalyst is not necessary. Another advantage of this fuel cell is the high conversion.

Properties and applications of all types of fuel cell are shown in table 2.1.

Table 2.1 Operating and applicable properties of five main types of fuel cells [3, 30].

Type of Fuel Cell	**Operating Temp (°C)**	**Power Density (mW/cm^2)**	**Fuel Efficiency (Chem. to Elec.)**	**Lifetime (hr)**	**Capital Cost ($/kW)**	**Area of Application**
AFC	60-90	100-200	40-60	>10,000	>200	Space, Mobile
PAFC	160-220	200	55	>40,000	3000	Distributed Power
PEMFC	50-80	350	45-60	>40,000	>200	Portable, Mobile, Stationary
MCFC	600-700	100	60-65	>40,000	1000	Distributed Power Generation

Table 2.1 Operating and applicable properties of five main types of fuel cells [3,30].

Type of Fuel Cell	Operating Temp (°C)	Power Density (mW/cm^2)	Fuel Efficiency (Chem. to Elec.)	Lifetime (hr)	Capital Cost ($/kW)	Area of Application
SOFC	800-1000	240	55-65	>40,000	1500	Baseload Power Generation

2.2 Proton Exchange Membrane Fuel Cells (PEMFCs)

The proton exchange membrane fuel cells are the most usable types of fuel cells because of low operating temperature, high efficiency, long lifetime, low cost and zero emission [3].

2.2.1 Type of Proton Exchange Membrane Fuel Cells

2.2.1.1 Low Temperature Proton Exchange Membrane Fuel Cells

Low temperature proton exchange membrane fuel cell (LT-PEMFC) is a simple type of proton exchange membrane fuel cells. Its operating temperature is around 50-80 °C [3, 31]. Perfluorocarbon sulfonic acid (PFSA) or Nafion is a membrane used in this type of fuel cell and platinum is commonly used as a catalyst. There are only two types of fuels: hydrogen and oxygen. The operation generates only water so there are no problems about pollution. Moreover, it gains high power density as shown in table 2.1. However, it has a drawback about water generated from the reactions. Water

generated more cause flooding problem which reduces efficiency of the cell so water management system is important [32].

2.2.1.2 High Temperature Proton Exchange Membrane Fuel Cells

High temperature proton exchange membrane fuel cell (HT-PEMFC) is another type of fuel cells which discovered recently. Its operating temperature is about 120-200 °C. Water management system is not required because water is not in liquid form in this high temperature operation. Heat generated from the operation can remove water efficiently. Moreover, it can tolerate carbon monoxide at high temperature. Several type of polymer used as electrolyte such as inorganic-organic composite membrane, sulfonated hydrocarbon polymer membrane, membrane of blend polymers and acid-based polymer membrane. However, its power density is lower than low temperature proton exchange membrane fuel cell [32].

2.2.2 Construction of Proton Exchange Membrane Fuel Cells

Proton exchange membrane fuel cells are composed of membrane electrode assembly (MEA), bipolar plates and current correctors [10]. Structure of this fuel cell is shown in figure 2.1.

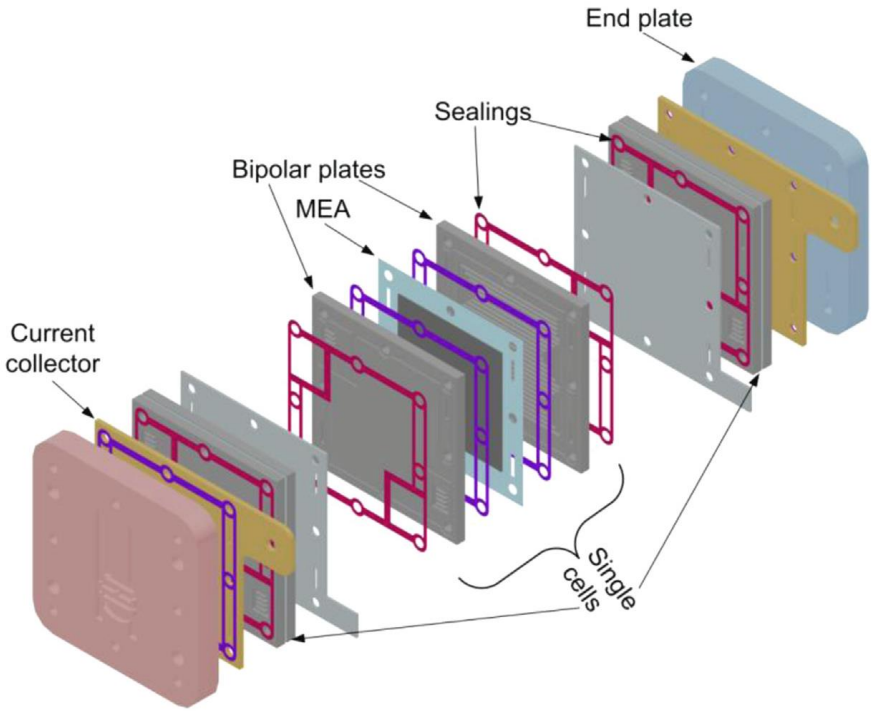

Figure 2.1 Construction of single PEM fuel cell [2].

The central part of the cell called membrane electrode assembly is the most important part of the cells [4]. It consists of proton exchange membrane (PEM) and two electrodes named anode and cathode. Proton exchange membrane is a polymeric thin film act as an electrolyte. The membrane is used to prevent direct contacting of anode and cathode. It allows only protons to pass through so electrons flow outside the cell and provide energy. Its surface was coated by a catalyst made from platinum. Two types of electrode, anode and cathode are the layers where electrochemical reactions occur. Construction of MEA is shown in figure 2.2.

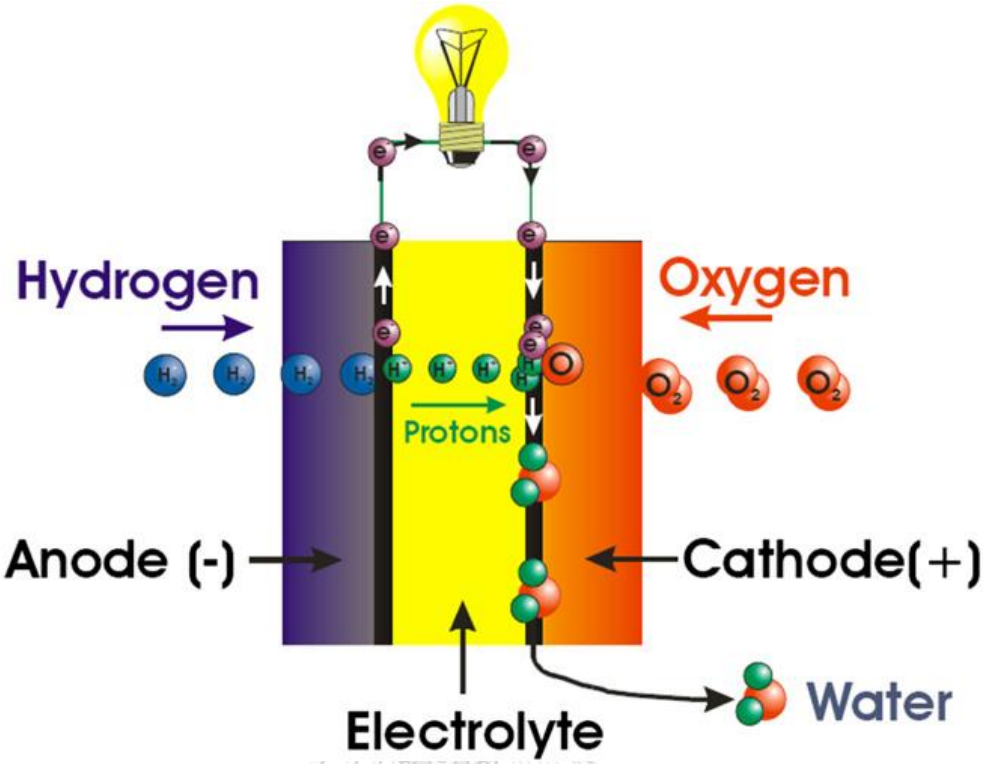

Figure 2.2 Schematic design of the membrane electrode assembly [12].

Bipolar plates are the important component in this type of fuel cell. They have about 60-80% weight of fuel cell and 30-40% of overall cost [6-8].

Current collectors are the component which collect electricity and bring it out of the cell.

2.2.3 Operation of Proton Exchange Membrane Fuel Cells

The operation starts when hydrogen is fed to the anode side of the cell. At the anode, hydrogen releases two electrons and remains two protons. This reaction called oxidation reaction.

$$H_2 \rightarrow 2H^+ + 2e^-$$

The electrons are blocked by the polymeric electrolyte membrane so they flow out of the cell to generate energy. Only protons can penetrate the electrolyte to the cathode side

The oxygen is fed to the cathode side. At the cathode, oxygen reacts with protons and electrons from anode to form water called reduction reaction.

$$O_2 + 4H^+ + 4e^- \rightarrow 2H_2O$$

2.3 Bipolar Plates

Bipolar plates or backplates [4] have multiple functions such as 1) separate one unit of fuel cell from other cells in the stack; 2) withstand external force; 3) manage internal water generated from electrochemical reactions; 4) remove heat out of the cell; 5) distribute fuel and oxygen within the cell; 6) bring current out of cell; 7) provide good conductivity between cathode side of the cell and anode side of adjacent cell [4, 8-11].

To develop bipolar plates which suitable for all applications as mention, material must have high flexural strength and modulus to withstand external force, have several pathways to bring water out as shown in figure 2.3, be hydrophobia or have low water absorption, have high through-plane thermal conductivity to remove heat out of cell, have high in-plane electrical conductivity to bring current out of the

cells, have high corrosion resistance to withstand fuel and water and have flow channels to distribute fuel as shown in figure 2.4.

US Department of Energy (DOE) specified targets of bipolar plates which required several specifications as shown in table 2.2.

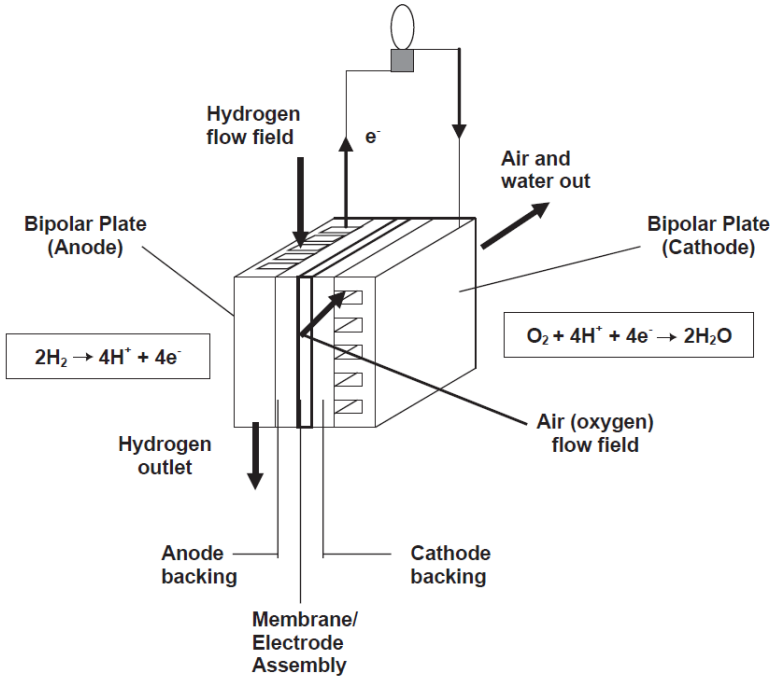

Figure 2.3 Diagram of PEMFC showed port of fuel and water [10].

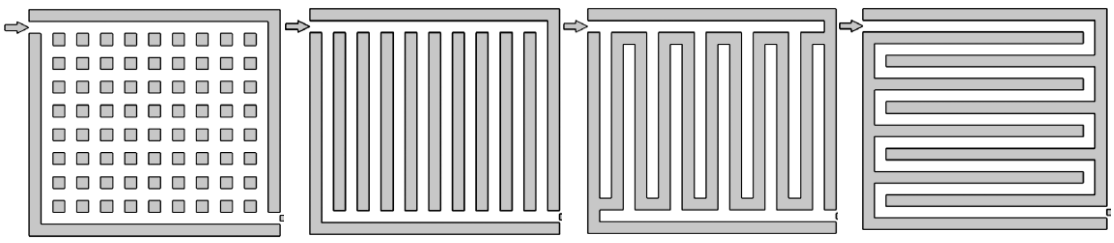

Figure 2.4 Schematic drawing of different types flow field channels on bipolar plate a) pin-type flow field. b) parallel channels flow field. c) interdigitated flow field. d) single serpentine flow field [33].

Table 2.2 Properties of bipolar plate required by DOE [11-14].

Characteristic	**Units**	**2010**	**2020**
Electrical Conductivity	S/cm	>100	>100
Thermal Conductivity	W/m·K	>10	>20
Flexural Strength	MPa	>25	>25
Corrosion, anode	$\mu A/cm^2$	<1	<1
Corrosion, cathode	$\mu A/cm^2$	<1	<1
Water absorption	% at 24 h.	<0.3	<0.3
Plate H_2 permeation	Std. cm^3 / sec cm^2 Pa at 80^OC	$<2x10^{-6}$	$<1.3x10^{-14}$
Cost	$/kW	5	3
Weight	kg/kW	<0.4	-

The materials used to make bipolar plates are classified to three types: non-metals; metals; and polymer composites [10] as shown in figure 2.5.

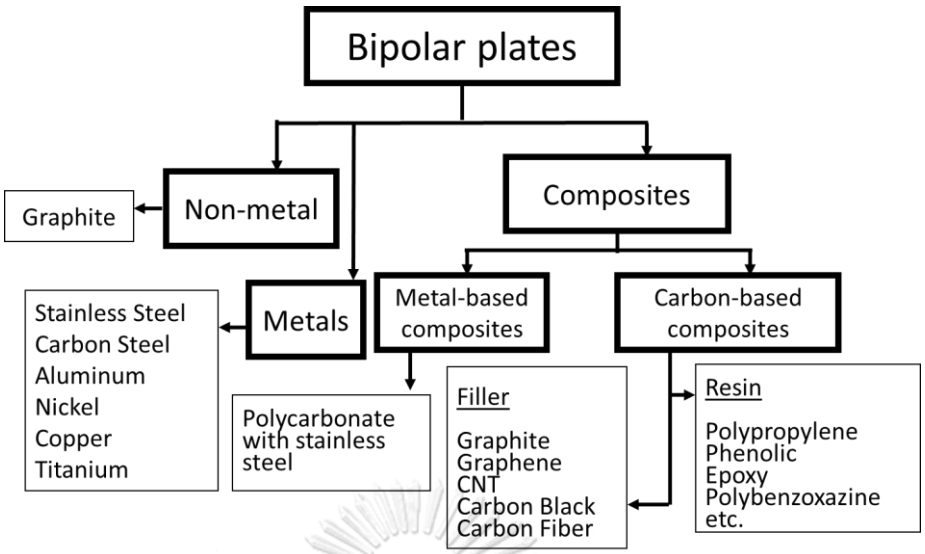

Figure 2.5 Classification of materials for bipolar plates used in PEMFCs.

2.3.1 Metallic Bipolar Plates

Several types of metals were used to be material for bipolar plates [10]. They have many advantages such as high mechanical strength, high conductivity, easy to processing and easy to stamp to create flow channel. Metallic bipolar plates can be classified to three types: precious non-coated, non-coated and coated metallic bipolar plates.

2.3.1.1 Precious Non-coated Metal Bipolar Plates

All metals used in this type of bipolar plates are noble metals such as gold and platinum [34]. They have excellent mechanical, thermal and electrical properties but they have too high cost to use in commercial scale.

2.3.1.2 Non-coated Metal Bipolar Plates

Metals used as non-coated bipolar plates are stainless steels, aluminum, titanium and nickel [10, 34]. They also have high mechanical properties, high thermal properties, high chemical stability, low gas permeability and low cost [10, 35]. However, they have a problem about contact resistance in oxide layer produced from corrosive process. Recently, austenitic and ferritic stainless steel were developed for bipolar plates to improve contact resistance [36].

2.3.1.3 Coated Metal Bipolar Plates

To overcome corrosion problem, coated metals are used as bipolar plates. Aluminum, stainless steel and nickel are chosen as alternatives for coating. Coatings must have high thermal conductivity, high electrical conductivity and good adhesion with the substrates. There are two types of coatings: carbon-based coating and metal-based coating. Graphite, diamond like carbon, organic self-assembled monopolymers and conductive polymer are example of carbon-based coating. The other types of coating such as metal-based coatings are consist of noble metals, metal nitrides and metal carbides [10, 34, 36].

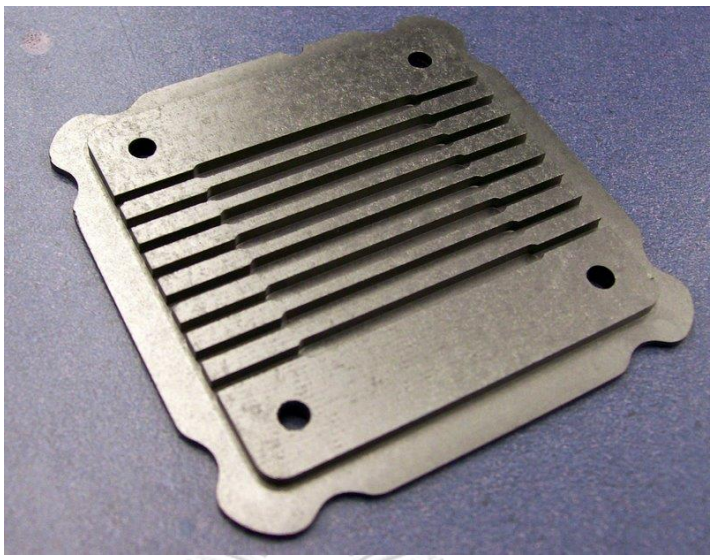

Figure 2.6 Metallic bipolar plate [37].

2.3.2 Non-metal Bipolar Plates

One of the most interesting material chosen to make non-metal bipolar plates is non-porous graphite gained by both natural and synthetic. Graphite is an allotrope of carbon which has high thermal conductivity, electrical conductivity, good chemical stability and low density. The bipolar plates made of graphite have high electrochemical power output. However, they have drawbacks about high cost, low mechanical strength and hard to processing [10, 34, 35, 38].

Figure 2.7 Graphite bipolar plate [1].

2.3.3 Polymer Composites Bipolar Plates

Polymer composites are the other alternatives for bipolar plates. There are advantages in low weight and can be molded in any size or shape [10]. There are two types of fillers used in the composites: metal and carbon.

2.3.3.1 Metal-based Composite Bipolar Plates

Only type of metal used to fill in the composites is stainless steel. Polycarbonate filled with graphite and stainless steel gains high rigidity, high chemical resistance and can be molded in any shape [8].

2.3.3.2 Carbon-based Composite Bipolar Plates

Carbon- based composites have several advantages such as low weight, corrosion resistance [38] and can be molded into several size and shape. Polymer has

a duty to hold fibers or fillers in suitable direction for increase properties of the plates. Both thermoplastic and thermoset can be used as resin for bipolar plates [8].

Several types of thermoplastic used to make bipolar plates such as polypropylene (PP), polyvinylidene fluoride (PVDF), polyphenylene sulfide (PPS) or polyether ether ketone (PEEK). These polymers have good mechanical properties [8].

Thermosetting used for bipolar plates have higher strength, lower viscosity and more toughness than thermoplastic. Moreover, they can be cured at temperatures higher than their glass transition temperatures. Examples of these types of polymers are epoxy, phenolic and vinylester (VE) [8].

Different types of carbon filled in the composites such as graphite, graphene, carbon nanotubes, carbon black and carbon fibers. Carbon-based composites can overcome drawbacks occurred in metal-based composite. Polymer-graphite composite is used as manufacturing bipolar plates [10].

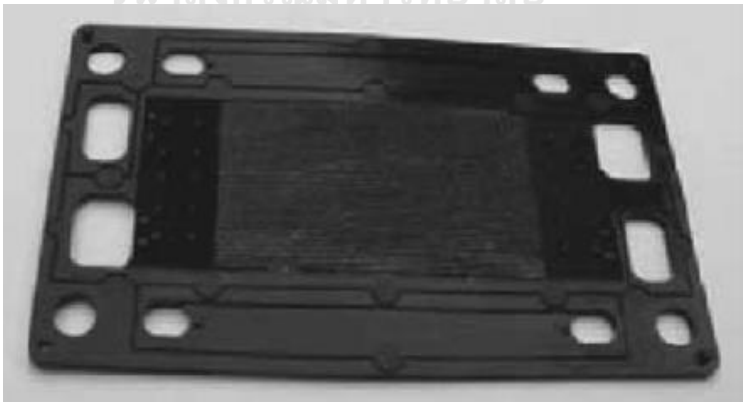

Figure 2.8 Graphite-polymer composite bipolar plate [39].

2.4 Graphite

The word “graphite” is derived from the Greek word “graphein” meaning “to write” because graphite have been used to write and draw for a long time. Graphite is an allotrope of carbon like diamond but it has different structure significantly. Graphite consists of a lot of parallel planes interact together. There are two type of planes: A plane and B plane which carbon atoms are not neighbor directly. Each plane consists of two types of carbon atom: alpha-atom which has direct neighbors above and below the adjacent plane and beta-atom which has not direct neighbor. Every atom in plane is bonded with three other atoms look like hexagonal shape with covalent bond as shown in figure 2.9.

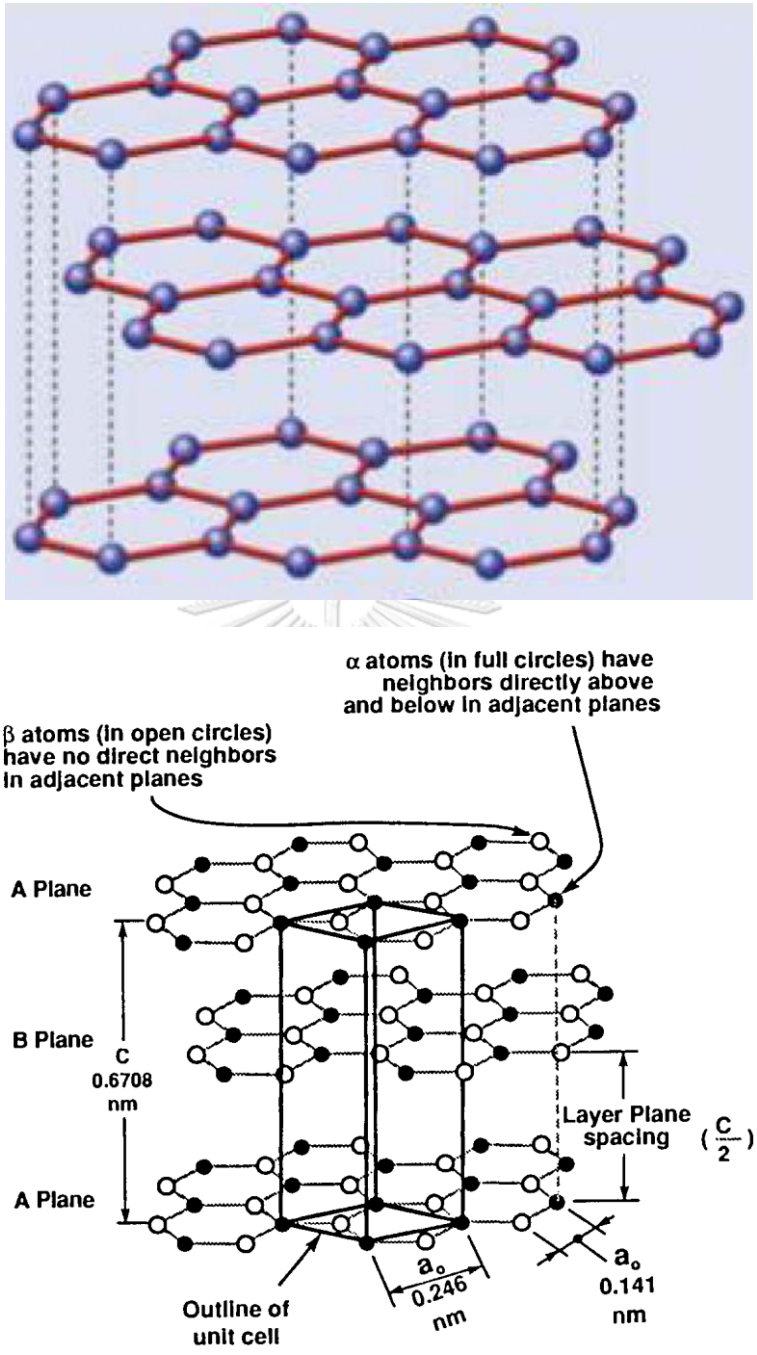

Figure 2.9 Crystal structure of graphite [40, 41].

There are two main types of graphite i.e. natural and synthetic. Natural graphite can be found as a mineral in nature while synthetic graphite was prepared by heating

unstructured carbon at high temperature in which it shows lower impurity than natural graphite [42, 43]. Graphite has outstanding properties as shown in table 2.3.

Table 2.3 Properties of graphite [8, 41, 44, 45].

Properties	Values
Physical Properties	
Density (g/cm^3)	1.8 – 2.26
Color	black
Aspect ratio	close to 1
Specific surface area (m^2/g)	6.5 – 20
Water absorption (%)	0.5 – 3.0
Mechanical Properties	
Flexural strength (MPa)	10 – 100
Flexural modulus (GPa)	5 - 10
Thermal Properties	
Specific heat capacity (J/g·K)	0.69 - 0.719
Thermal conductivity (W/m·K)	300 - 600
Coefficient of thermal expansion	8.39
Thermal shock resistance (^{o}C)	200 - 250
Electrical Property	
Electrical conductivity (S/cm)	2.5 x 10^4

2.5 Graphene

Graphene was discovered in 2004 by Prof. Andre Geim and Prof. Konstantin Novoselov from University of Manchester [46]. Graphene is synthesized from graphite by plenty of methods. The simplest method called micromechanical exfoliation of graphite or scotch tape method [40]. Others method such as chemical vapor deposition (CVD), chemical conversion, reduction method, separation or exfoliation of graphite or graphite oxide and arc discharge [47]. The definition of graphene is a single atomic plane of sp^2 bound carbon [48]. Graphene is a two- dimensional (2- D) nanomaterial which has flake shape as thick as one unit of graphite. The structure of graphene is shown in figure 2.10.

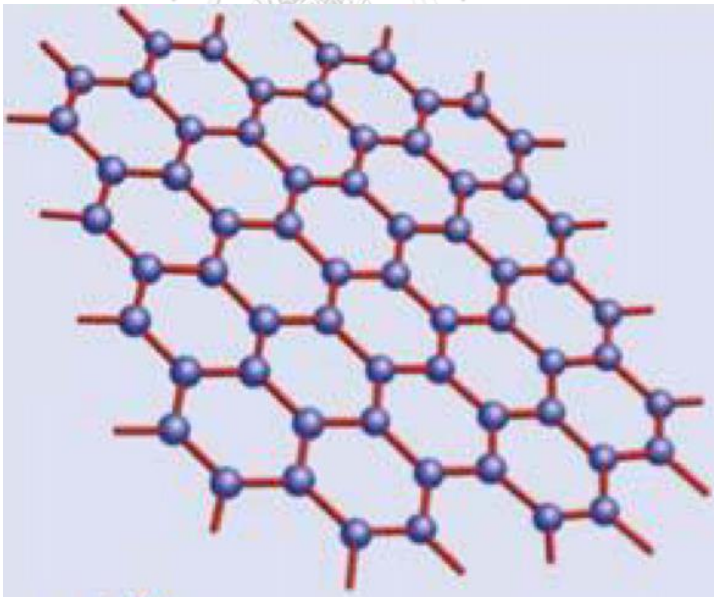

Figure 2.10 Crystal structure of graphene [40].

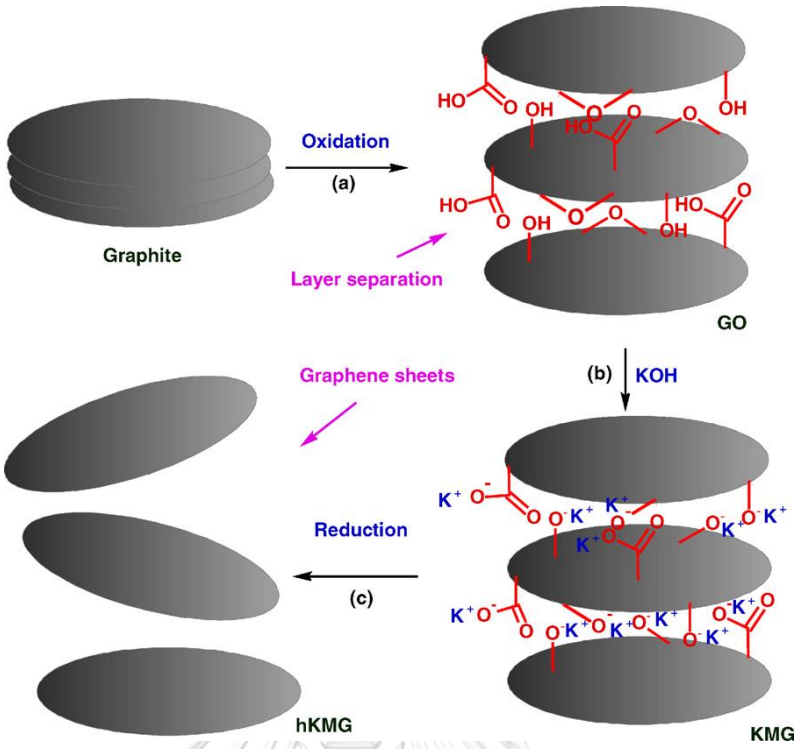

Figure 2.11 A simple route for the preparation of graphene from graphite by reduction method [40].

Graphene is one of nanomaterial which has superb properties. The properties of graphene are shown in table 2.4.

Table 2.4 Properties of graphene [8, 44, 47, 49].

Properties	Values
Physical Properties	
Density (g/cm^3)	2.2
Color	Black
Length (μm)	50

Table 2.4 Properties of graphene [8, 44, 47, 49].

Properties	Values
Physical Properties	
Thickness (nm)	1 - 35
Aspect ratio	1,400 - 50,000
Specific surface area (m^2/g)	2,630
Mechanical Properties	
Tensile strength (GPa)	130
Tensile modulus (TPa)	1
Thermal Properties	
Specific heat capacity (J/g·K)	1.076
Thermal conductivity (W/m·K)	2,000 - 6,000
Coefficient of thermal expansion	1×10^{-6}
Electrical Property	
Electrical conductivity (S/cm)	2×10^{4}

2.6 Carbon Nanotubes (CNTs)

Carbon nanotube (CNTs) is another type of carbon along with graphite, graphene, fullerene or diamond. They were discovered in 1991 by a Japanese researcher named Sumio Iijima [50]. Carbon nanotubes are known as one-dimensional

(1D) nanomaterials while fullerene is zero-dimensional (0-D) nanomaterial, graphene is two- dimensional (2- D) nanomaterial, graphite and diamond are called three-dimensional (3- D) material. They can synthesized by rolling graphene sheet into cylinders. Nowadays, a lot of method used to produce carbon nanotubes such as chemical vapor deposition (CVD), laser method, arc discharge method or ball milling method [51].

Carbon nanotubes have tubular structures which 1 – 50 nm diameter and a few micron to centimeter length. Their structures were shown in figure 2.12.

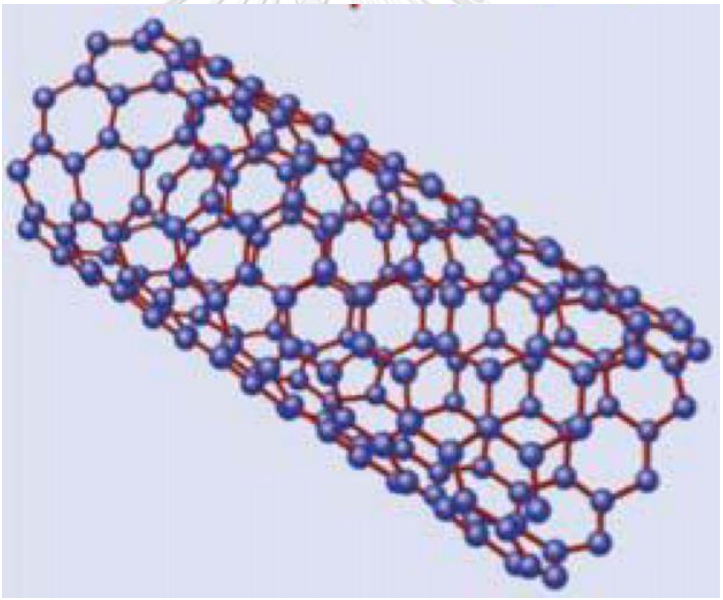

Figure 2.12 Crystal structure of carbon nanotubes [40].

There are two main types of carbon nanotubes i.e. single- walled carbon nanotubes (SWCNTs) and multi-walled carbon nanotubes (MWCNTs) [8, 50-52]. Single-walled carbon nanotubes have only layer of one- atom graphene. This type of nanotubes has high mechanical, thermal and electrical properties along with high cost.

Multi-walled carbon nanotubes have more than two layers of graphene rolled into cylinders with lower cost than SWCNTs. Double-walled carbon nanotubes (DWCNTs) are also a special type of multi-walled carbon nanotubes which have only two layers of graphene. The structures of SWCNTs and MWCNTs are shown in figure 2.13.

SWCNTs and MWCNTs have different properties. SWCNTs have better electrical properties than MWCNTs. However, SWCNTs may contain imperfection showed by micrographs [53]. SWCNTs usually be used in electronic devices such as field effect transistors (FETs) or logic gate. MWCNTs can carry high current density and have higher Young's modulus than SWCNTs [52, 54, 55].

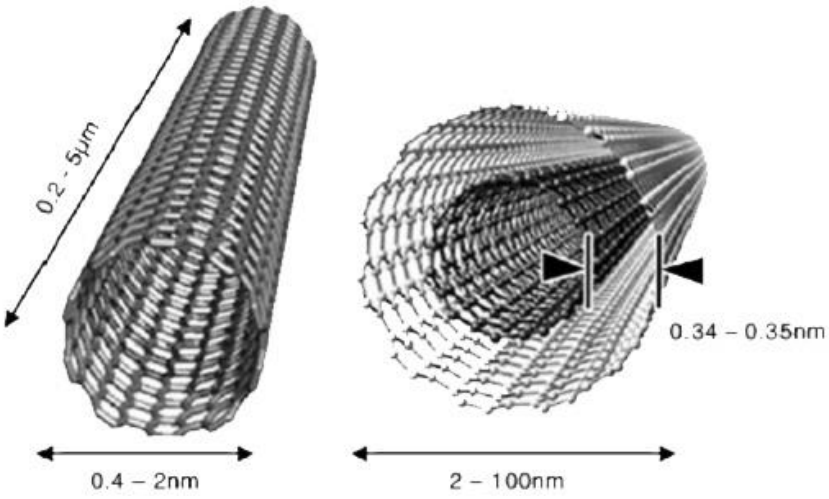

Figure 2.13 Diagram of single-walled carbon nanotubes (left) and multi-walled carbon nanotubes (right) [56].

Carbon nanotubes have interesting properties as shown in table 2.5.

Table 2.5 Properties of carbon nanotubes [8, 44, 50-52, 57, 58].

Properties	Values
Physical Properties	
Density (g/cm^3)	1.8 - 2
Color	Black
Length (μm)	1 – 18 x 10^6
Diameter (nm)	1 - 50
Aspect ratio	1,000 - 50,000
Specific surface area (m^2/g)	10 - 250 m^2/g
Tensile strength (GPa)	60 – 150
Tensile modulus (TPa)	0.2 – 1
Thermal Properties	
Specific heat capacity (J/g·K)	0.75 – 1
Thermal conductivity (W/m·K)	3,000 – 3,500
Coefficient of thermal expansion	1 x 10^{-6}
Electrical Property	
Electrical conductivity (S/cm)	3,000 - 4,000

2.7 Polybenzoxazine

Polybenzoxazine is a novel type of thermosetting developed from phenolic resin to overcome its drawback. Benzoxazine resins are synthesized by mixing phenol, aldehyde and amine functional group together by using solvent or solventless technique [59]. Polybenzoxazine can be polymerized by open the oxazine ring of benzoxazine monomer. This new thermosetting has many important advantages such as good mechanical properties, high glass transition temperature, low water absorption, high char yield, no catalyst used for synthesizing, no by-product gained from curing and near zero shrinkage [15, 16, 18-20, 59, 60].

Benzoxazine resins can be classified into several types based on theirs mixtures. Bisphenol-A and aniline based benzoxazine is the most popular type of benzoxazine resin because of their very low viscosity and good thermal properties [60]. Their properties are shown in table 2.6.

The most important property of polybenzoxazine for apply as matrix in composite is its low melt viscosity about 5 Pa.s at temperature of 80°C. This type of polymer can coat filler thoroughly so large amount of filler can filled in the composite.

Table 2.6 Properties of polybenzoxazine [16, 59, 61].

Properties	Values
Mechanical Properties	
Storage Modulus at 25 °C (GPa)	2.2
Tensile Modulus (GPa)	5.2
Tensile Strength (MPa)	64
Flexural Modulus (GPa)	4.5
Flexural Strength (MPa)	126
Physical Properties	
Monomer Density (g/cm^3)	1.2
Polymer Density (g/cm^3)	1.195
Water Absorption (% at 25 °C 24 h)	0.11
Thermal Properties	
Curing temperature (°C)	160 - 220
Glass transition temperature (°C)	150 - 180
Degradation temperature at 5% weight loss (°C)	310
Char yield (%)	32

Bisphenol-A based benzoxazine resin can be synthesized using solventless process disclosed by Ishida [15, 60]. This process is carried out by mixing bisphenol-A,

paraformaldehyde, and aniline at 1:4:2 molar ratio at temperature of 110 °C. The synthesize path is shown in figure 2.14. Polymerization process or curing process of polybenzoxazine is proceeded by heating the monomer to open its cyclic ring. The formation of polybenzoxazine is shown in figure 2.15.

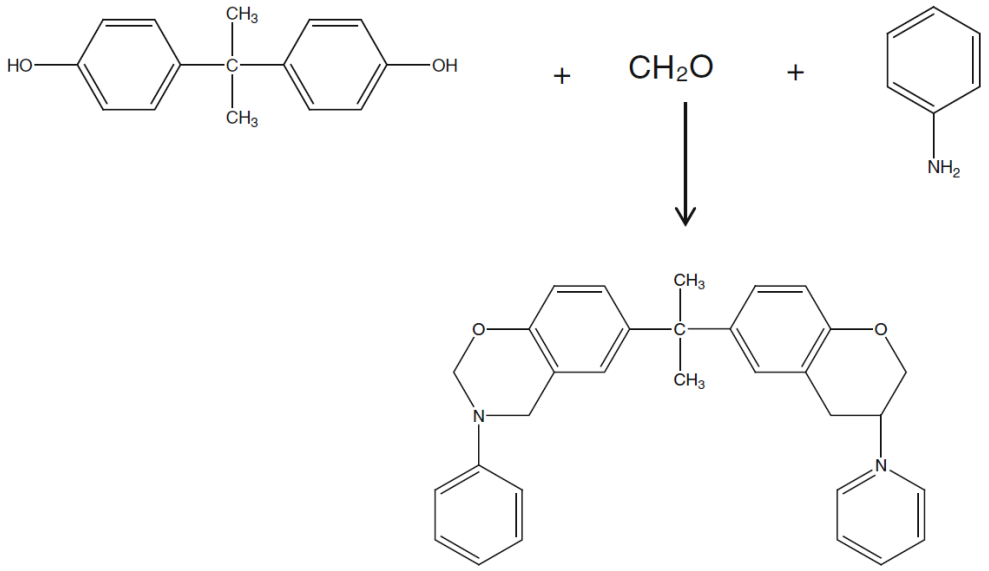

Figure 2.14 Synthesize path of BA-a [60].

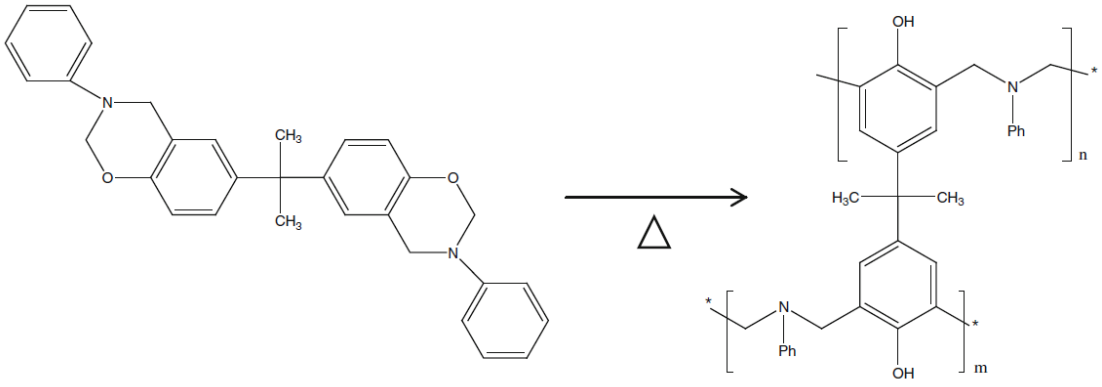

Figure 2.15 Formation of polybenzoxazine by thermal curing process [60].

CHAPTER III

LITERATURE REVIEWS

H. Ishida and S. Rimdusit (1998) [17] developed highly-filled boron nitride-polybenzoxazine composites to obtain very high thermal conductivity. Highly thermal conductivity could be obtained by adding maximum content of filler as soon as possible. They synthesized composite of polybenzoxazine and boron nitride. The highest content of boron nitride filled in the composite was 78.5% by volume or 88% by weight. Thermal conductivity was supremely increased to 32.5 W/m·K as shown in figure 3.1. The high content of boron nitride was possible because large particle size of boron nitride caused less specific surface area. Moreover, low melt viscosity of benzoxazine could wet whole area of boron nitride particle with good adhesion.

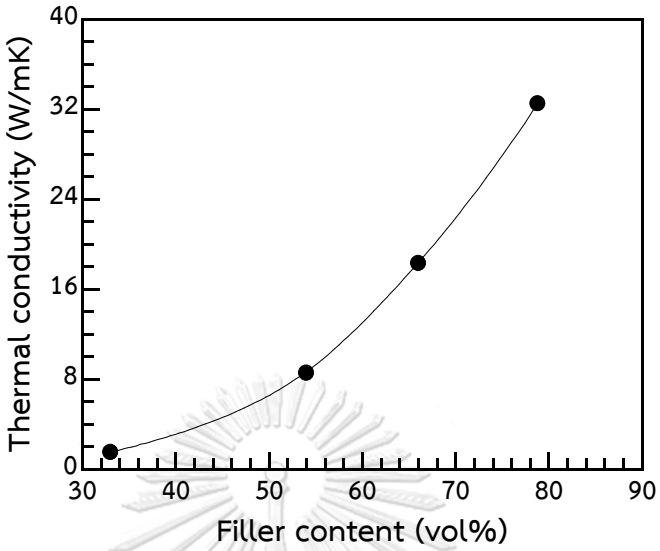

Figure 3.1 Thermal conductivity of boron nitride-filled polybenzoxazine as a function of filler contents [17].

I. Dueramae, A. Pengdam and S. Rimdusit (2013) [21] were accomplished to use highly filled graphite polybenzoxazine composites. Figure 3. 2 shows thermal conductivity of graphite polybenzoxazine composites at 25 °C with different graphite content. The highest graphite content filled in composite was 80 wt%. Thermal conductivity of the composite was improved from 0.23 W/m·K of neat benzoxazine to 10. 2 W/ m·K or about 44 times. They found that increasing graphite content could increase thermal conductivity rapidly because graphite had high thermal conductivity and could construct significant conductive pathway in the composites. Department of Energy, USA (DOE) gave the recommended value of thermal conductivity of bipolar plate for PEMFCs at 10 W/m·K so polybenzoxazine composite with 80 wt% graphite has higher thermal conductivity than the requirement set by Department of Energy.

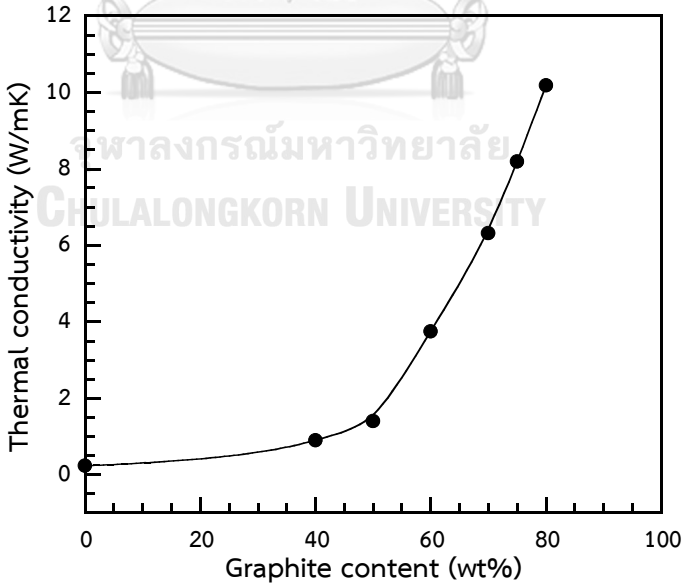

Figure 3.2 Thermal Conductivity at 25 °C of graphene and graphite filled polybenzoxazine as a function of filler contents [21].

R. Plengudomkit, M. Okhawilai and S. Rimdusit (2014) [7] developed polybenzoxazine composite filled with graphene. They found that the maximum graphene content filled in the composite was 60 wt%. Increasing graphene content also improved thermal conductivity in the composites. Filling 60 wt% graphene could increase thermal conductivity to 8.03 W/m·K as shown in figure 3.3. Highly thermal conductivity could be obtained because formation of conductive network in graphene could reduce heat resistance in the composite. This composite has higher thermal conductivity than graphite polybenzoxazine composite developed by Dueramae *et al.* [21] at the same filler content. They were found that smaller particle size and higher aspect ratio of graphene could form greater conductive network than graphite.

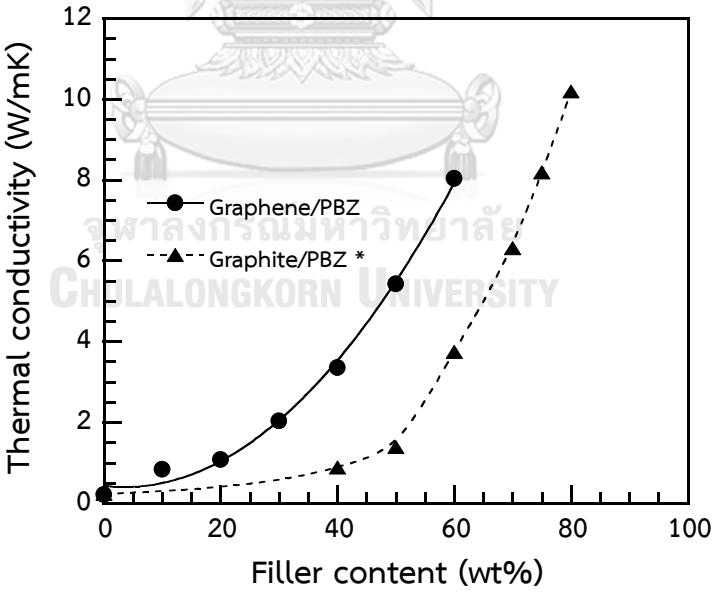

Figure 3.3 Thermal conductivity at 25 °C of graphene and graphite filled polybenzoxazine as a function of filler contents [7].

M. Phuangngamphan (2016) [29] developed highly-filled graphite and graphene polybenzoxazine composites. She found that graphite with large particle size could be filled in polybenzoxazine composite as high as 83 wt% as shown in table 5.1 because large particle of fillers had lower surface area than small particle of fillers. For this reason, largest particle size of graphite was used in this research. Then, graphite and graphene were filled in polybenzoxazine composite with total content at 83 wt%. Figure 3.4 illustrates thermal conductivity of polybenzoxazine composites filled with graphite and graphene at room temperature with different graphite and graphene content. It was found that the optimal graphene content was 7.5 wt% and the highest thermal conductivity was 14.5 W/m·K. Adding little amount of graphene could improve thermal conductivity because graphene has higher intrinsic thermal conductivity [8, 44, 47, 49] and smaller particle size than graphite. Graphene could fill the void between particles of graphite to generate greater thermal conductive pathway. However, adding large amount of graphene caused too large surface area and agglomeration of filler.

Table 3.1 The effect of particle size on composite packing densities [29].

Average particle size (μm)	Type	Maximum loading (wt%)
<50	Aggregate	75
140	Aggregate	80
240	Aggregate	83

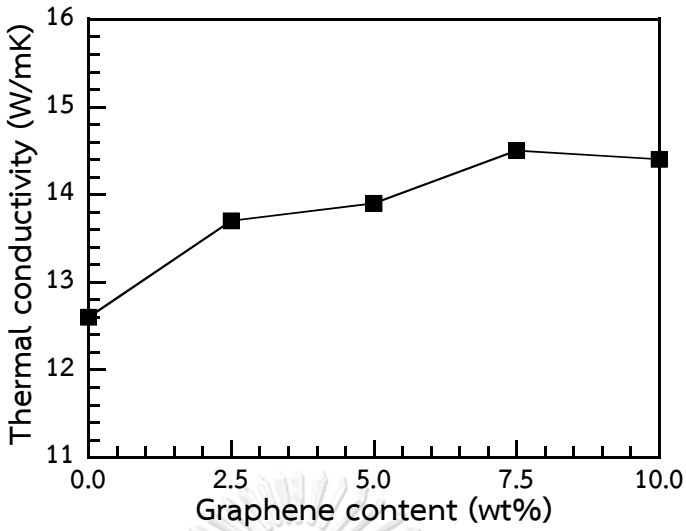

Figure 3.4 Thermal conductivity at 25 °C of graphite/graphene filled polybenzoxazine composites as a function of graphene contents [29].

S. R. Dhakate (2010) *et al.* [25] developed phenolic composites filled with graphite and multi-walled carbon nanotubes. They added graphite in phenolic resin at maximum content of 65% by volume. Phenolic composite filled with 65 vol% of graphite had thermal conductivity at 1 W/m·K for through-plane direction and 13 W/m·K for in-plane direction. Then, they filled multi-walled carbon nanotubes at different contents. Figure 3.5 illustrates thermal conductivity of carbon nanotubes and graphite phenolic composites at different contents of carbon nanotubes. It was found that adding small amount of multi-walled carbon nanotubes increased thermal conductivity of the composite due to high intrinsic thermal conductivity, orient in all direction and high aspect ratio of carbon nanotubes could bridge the space between particles of graphite [8]. However, filling too large amount of carbon nanotubes caused agglomeration phenomenon. In this research, the optimal content of multi-walled carbon nanotubes was 1 % by volume. The thermal conductivity was increased from 1 W/m·K to 13 W/m·K for through-plane direction and from 25 W/m·K to 50 W/m·K for in-plane direction. The through-plane thermal conductivity are lower than the in-plane thermal conductivity because high aspect ratio of multi-walled carbon nanotubes cause anisotropy effect on thermal conductivity. This effect is similar to the anisotropy effect of graphite nanoplatelet with high aspect ratio on polymer composite [62]. However, total content of fillers filled in phenolic composite are 65 wt% because phenolic resin has higher viscosity than benzoxazine resin [63].

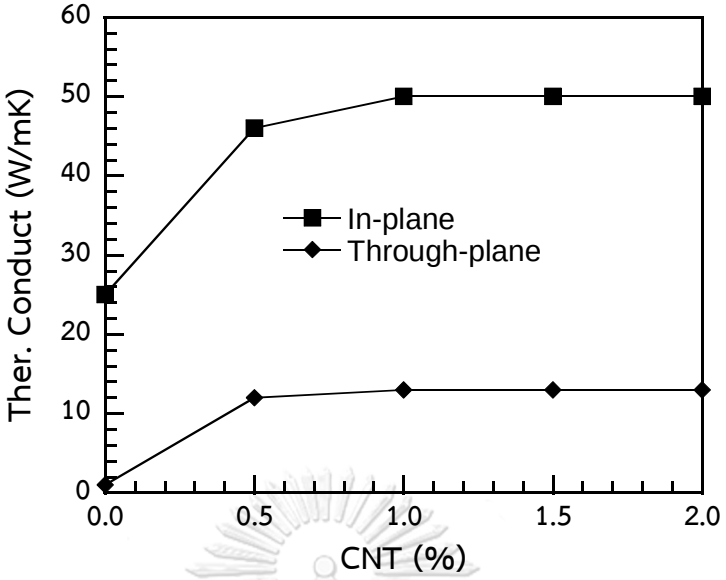

Figure 3.5 Thermal conductivity with increasing MWCNTs vol% in graphite–polymer composites [25].

A. Yu *et al.* (2008) [64] developed epoxy composites filled with graphite nanoplatelet (GNP), another type of carbon nanomaterial which is thicker than graphene [48] and single-walled carbon nanotubes (SWCNTs). Overall fillers filled in the epoxy composites were constant at 10 % by weight. Figure 3.6 illustrates thermal conductivity of the hybrid graphite nanoplatelet – carbon nanotubes epoxy composites. At GNP: SWCNTs filler ratio of 3:1, thermal conductivity reached the highest value and higher than epoxy filled with only GNP or only SWCNTs. This research confirmed strong synergistic effect between GNP and SWNT. This synergism occurs because flexible SWCNTs bridged the planar of graphite nanoplatelets and decreased thermal interface resistance.

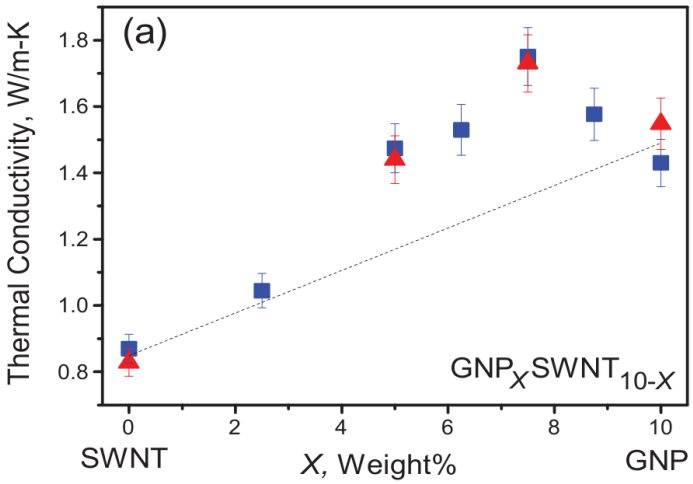

Figure 3.6 Thermal conductivities of epoxy composites prepared with hybrid GNPxSWCNTs10-X filler as a function of GNP filler percentage (x); the total filler loading is maintained at 10 wt %. Dashed line corresponds to the change of thermal conductivity expected from the rule of mixtures. Triangles and squares in (a) and (b) correspond to two independent sets of composite sample preparation [64].

T. Lu *et al.* (2017) [65] developed hybrid composite of high-density polyethylene (HDPE) filled with multiwalled carbon nanotubes and few-layered graphene. Thermal conductivity of single composites and hybrid composites at filler contents of 0-4.3 vol% were shown in figure 3.7. They found that thermal conductivities of the hybrid filler composites were higher than thermal conductivities of the single filler composites for all filler contents. This phenomenon occurred because both carbon nanotubes and graphene have large specific surface area, high aspect ratio and high thermal conductivity. Moreover, they provided good dispersion in polymer matrix. Graphene could make contact with two adjacent carbon nanotubes to generate a conductive network path which increase thermal conductivity significantly.

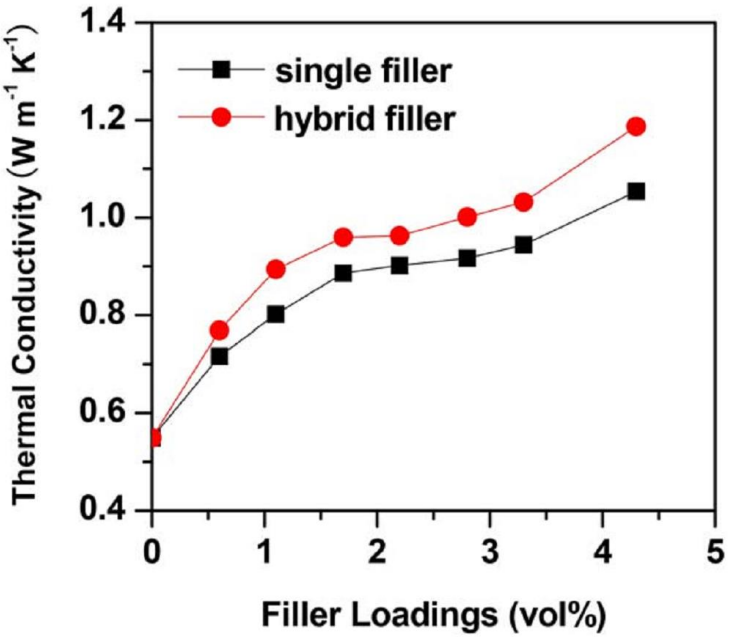

Figure 3.7 Thermal conductivity as functions of filler loading for the HDPE-based composites with the single and hybrid filler, respectively [65].

J. Che *et al.* (2017) [66] studied synergistic effect on high density polyethylene filled with expanded graphite and carbon nanotubes. Electrical conductivity of the composites were measured and shown in figure 3.8. It was found that percolation effect was occurred in both carbon nanotubes filled composite and expand graphite filled composite. Carbon nanotubes filled composite had less percolation threshold and higher conductivity than expand graphite filled composite. This result showed that conductive network formed by carbon nanotubes was denser than network formed by expand graphite. Moreover, the ternary system composite of polyethylene, carbon nanotubes, and expanded graphite were developed. It was shown that adding small amount of carbon nanotubes on expanded graphite/polyethylene composites caused large enhancement of electrical conductivity too.

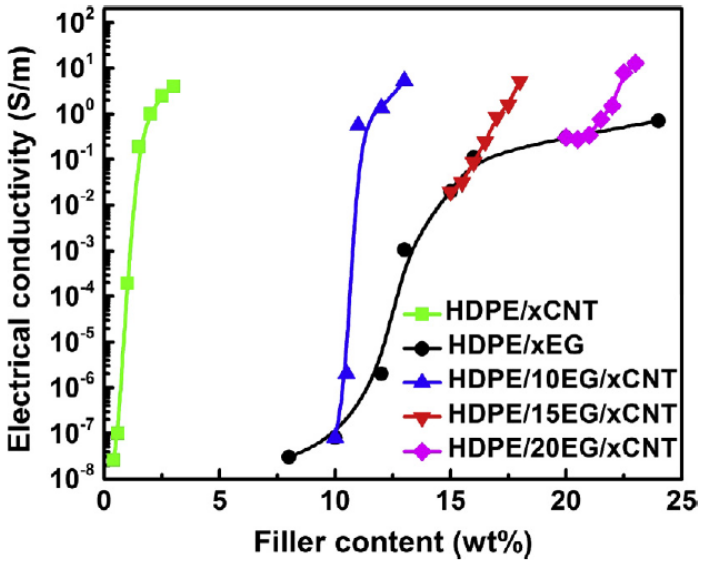

Figure 3.8 Electrical conductivity of HDPE/ EG/ CNTs ternary composites with maintaining the EG content at 10 wt%, 15 wt%, 20 wt% and increasing the filler content of CNT [66].

M. R. Zakaria *et al*. (2017) [67] compared properties of epoxy filled with graphene nanopowder and epoxy filled with multi- walled carbon nanotubes. Mechanical properties of the epoxy nanocomposites were illustrated in figure 3.9. The figure showed that epoxy filled with carbon nanotubes had higher flexural strength and flexural modulus than epoxy filled with graphene nanopowder at the same filler content. There are three reason for this phenomenon. First, graphene nanopowder had larger surface area and was more easily aggregated. Second, carbon nanotubes had weaker Van der Waals' force between theirs adjacent particle caused they disperse in matrix easily. Last, two- dimensional structure of graphene nanopowder caused it easily to detach from the matrix. The epoxy composite filled with 1 wt% carbon nanotubes provided the highest flexural strength (126. 70 MPa) and flexural modulus (3.35 GPa). Filling more than 1wt% of fillers could decrease mechanical properties due to the agglomeration of the fillers.

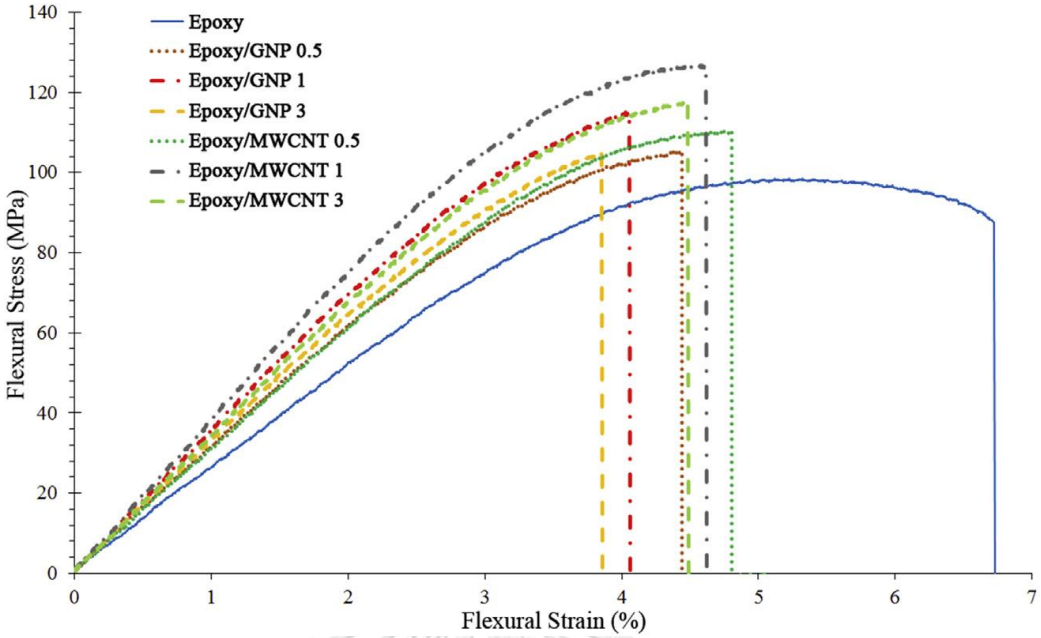

Figure 3.9 Flexural stress-strain curves of a neat epoxy and the epoxy composites with 0.5%, 1%, and 3% weight percentage of GNP and MWCNT [67].

CHAPTER IV

EXPERIMENTAL

4.1 Materials

There are four materials used in this research: benzoxazine resin (BA-a), synthetic graphite, graphene and multi-walled carbon nanotubes. Benzoxazine resin is based on bisphenol-A, para-formaldehyde and aniline. Bisphenol-A (AR grade) was obtained from PTT Phenol Company Limited. Paraformaldehyde (AR grade) and aniline (AR grade) were purchased from Merck Company and Panreac Quimica SA Company, respectively. Graphite was kindly supported from Toyo Tanso (Thailand) Company Limited. XGnP Graphene Nanoplatelets (Grade H) was bought from XG Sciences, USA. Carbon nanotubes were obtained from Nano Generation Company Limited.

4.1.1 Benzoxazine Synthesis

Benzoxazine resin was synthesized using three reactants i.e. bisphenol-A, para-formaldehyde and aniline by a solventless method [15]. First, bisphenol-A, para-formaldehyde and aniline were mixed at a 1:4:2 molar ratio and stirred continuously at 90-110^{o}C until it became light yellowish monomer. Then, the monomer was cooled to room temperature until it became yellow solid. Last, the monomer was ground into powder and kept in a refrigerator for future use. The density of this resin is 1.19 g/cm^{3}.

4.1.2 Graphite Characteristics

IG-70 graphite having density of 2.0 g/cm^3 was supplied by Toyo Tanso (Thailand) Co., Ltd. It has electrical resistivity, flexural strength, coefficient of thermal expansion, and coefficient of thermal conductivity of 10.0 uΩ.m, 47 MPa, 4.6x10^{-6} /K and 130 W/m·K, respectively [42].

4.1.3 Graphene Characteristics

XGnP Graphene Nanoplatelets (Grade H) which supplied from XG Sciences, USA has average diameter of 25 μm and 15 nm thickness with specific surface area of 60-80 m^2/g. The density of this material is 2.2 g/cm^3 [68].

4.1.4 Carbon Nanotubes Characteristics

Multi-walled carbon nanotubes were purchased from Nano Generation Company Limited. They have an average tube diameter and tube length of 10 nm and 80 μm, respectively with more than 90% purity. They have BET surface area of 250 m^2/g. Their density is also 2.0 g/cm^3 [69].

4.2 Specimen Preparation

First, all types of fillers were dried in oven at temperature of 100°C for 24 hours to get rid of moisture and kept in a desiccator at room temperature. Then, polybenzoxazine composites filled with graphite/graphene and carbon nanotubes were prepared by mixing benzoxazine resin, graphite, graphene and carbon nanotubes in an internal mixer with a constant speed rate of 40 rpm, a temperature of 90-100°C

for 30-45 minutes. The content of graphene was kept constant at 7.5wt% while the total content of graphite and carbon nanotubes were 76.5wt%. After achieved uniform-distributed mixture, the compounds were compressed using a compression molder with a pressure of 150 MPa, a temperature of 200°C for 3 hours to obtain fully-cured composites. Last, the composites were cut to an appropriate size and shape for further characterization.

4.3 Characterization Methods

4.3.1 Differential Scanning Calorimetry (DSC)

Curing characteristics of the composites were studied using a differential scanning calorimeter (model DSC1 Module) from Mettler-Toledo. All specimens were ground into small pieces about 5-10 mg and put in aluminum pans and sealed hermetically with aluminum lids. The experiments were heat using a heating rate of 10°C/min from 30°C to 300°C under nitrogen atmosphere at 50 ml/min. The curing temperatures were obtained from the peak of each thermogram while the heat of curing reactions were obtained from the areas under each exothermic peaks. The curing conversions were also calculated too.

4.3.2 Density Measurement

The density of each composites were examined by water displacement method (ASTM D792 Method A). All specimens were cut into rectangular shape with

dimension of 5cm × 2.5cm × 2mm. Weight of each specimen in air and water at 23±2°C was used to calculate density from equation 4.1.

$$\rho = \frac{A}{A - B} \times \rho_0 \quad (4.1)$$

Where ρ = density of each specimen (g/cm^3)

A = weight of specimen in air (g)

B = weight of specimen in water (g)

ρ_0 = density of water (g/cm^3)

Theoretical density of each specimen was calculated using equation 4.2.

$$\rho_c = \frac{1}{\frac{w_f}{\rho_f} + \frac{(1-w_f)}{\rho_m}} \quad (4.2)$$

Where ρ_c = theoretical density of each specimen (g/cm^3)

w_f = weight content of each filler (wt%)

ρ_f = density of each filler (g/cm^3)

ρ_m = density of the matrix (g/cm^3)

4.3.3 Dynamic Mechanical Analysis (DMA)

A dynamic mechanical analyzer model DMA242 from NETZSCH Instrument was used to characterize composites. The dimension of each composite was 5cm × 1cm × 2.5mm. The experiment was carried out using a three-point bending mode. A strain was applied in range of 0-30 μm at a frequency of 1 Hz. The temperature was scanned from 30-300°C with a heating rate of 5°C/min under nitrogen atmosphere. Storage

modulus (E') and loss modulus (E") were obtained from this characterization techniques. The glass transition temperature of each composite was also obtained from the temperature at the peak of the loss modulus curve.

4.3.4 Thermogravimetric Analysis (TGA)

Thermal stability of the composites were studied using a thermogravimetric analyzer (model TGA1 Module) from Mettler-Toledo. Specimens with weight of 5-10 mg were heat from 30°C to 850°C with a heating rate of 20°C/min under nitrogen atmosphere at a flow rate 50 ml/min. The thermal degradation temperature at 5% weight loss and char yield at 800°C of each specimen can determine from this type of thermogram.

4.3.5 Specific Heat Capacity Measurement

Specific heat capacity of each specimen was also examined by a differential scanning calorimeter (model DSC1 Module) from Mettler-Toledo. The specimens were put in aluminum pans and sealed hermetically with aluminum lids. The weight of each specimen was about 15-20 mg. The experiment was purged with dry nitrogen gas at a flow rate of 60 ml/min. The temperature was scanned from 15°C to 200°C with a heating rate of 1°C /min.

4.3.6 Thermal Diffusivity Measurement

Thermal diffusivity of the composites were investigated by laser flash diffusivity measurement (Nano-Flash-Apparatus, LFA 447, NETZSCH). The dimension of each composite was 10mm × 10mm × 1mm. The specimens were characterized at

atmosphere from room temperature to 180°C. The front side of specimens were heat by a short light pulse and the temperature at the rear side of specimens slightly increased. An infrared detector was used to detect the rising temperature and the thermal diffusivity was calculated using equation 4.3.

$$\alpha = \frac{kL^2}{t_{0.5}} \quad (4.3)$$

Where α = thermal diffusivity of each composite (mm^2/s)

k = the half-rise constant (0.13879 under ideal condition at half-rise)

L = thickness of the specimens (mm)

$t_{0.5}$ = the time for the rear face temperature to reach half of its maximum value

After thermal diffusivities of the composites were calculated, theirs thermal conductivities were calculated using equation 4.4.

$$k = \rho \times c_p \times \alpha \quad (4.4)$$

Where k = thermal conductivity of each composite (W/m·K)

ρ = density of each composite (g/cm^3)

c_p = specific heat capacity of composite (J/g·K)

α = thermal diffusivity of each composite (mm^2/s)

4.3.7 Electrical Conductivity Measurement

The electrical conductivity of composites was determined using four point probe technique (Lucas Labs S-302 with SP4 head) which connected to a source meter instrument (KEITHLEY 2410). The specimens were cut into 2 cm × 2 cm square shape.

The electrical conductivity of the composites was calculated using equation 4.5 and 4.6 [70, 71] and the five averaged value was reported.

$$\rho = \frac{V}{I} \times w \times \frac{\pi}{\ln 2} \times F \tag{4.5}$$

$$\sigma = \frac{1}{\rho} \tag{4.6}$$

Where ρ = volume resistivity (Ω·cm)

V = voltage (v)

I = current (A)

w = thickness of the specimens (cm)

F = correction factor (= 0.642 for 2 mm thickness specimens)

σ = electrical conductivity of the specimens (S/cm)

4.3.8 Flexural Properties Measurement

The flexural properties of each specimen were examined by a universal testing machine (model 5567) from Instron Instrument. The dimensions of all specimens were 5cm x 2.5cm x 2.5 mm. The experiment was carried out using three-point bending method with a support span of 32 mm. The crosshead speed used in this test was 0.85 mm/min. The flexural strength and flexural modulus were determined according to ASTM D790M. They were calculated using equation 4.7 and 4.8.

$$E_B = \frac{L^3 m}{4bd^3} \tag{4.7}$$

$$S = \frac{3PL}{4bd^2} \tag{4.8}$$

Where E_B = flexural modulus, MPa

S = flexural strength (MPa)

P = load at a given point on the load-deflection curve (N)

L = support span (mm)

b = width of the beam tested (mm)

d = depth of the beam tested (mm)

m = slope of the tangent to the initial straight-line portion of the load deflection curve (N/mm)

4.3.9 Water Absorption Measurement

Water absorption values were measure following ASTM D570. First, disked-shape specimens with diameter of 50 mm and thickness of 3 mm were dried in oven and weighed. Then, the specimens were submerged in distill water at room temperature for 24 hours. Next, wet the specimens, weigh and return it to the water bath. The water absorption values were calculated using equation 4.9.

$$\% \text{ Water absorption} = \left(\frac{W-W_d}{W_d}\right) \times 100 \quad (4.9)$$

Where W = weight of specimen at time t (g)

W_d = weight of dry specimen (g)

4.3.10 Scanning Electron Microscope (SEM)

A scanning electron microscope (SEM-EDS 6610LV) was used to study interfacial bonding between polybenzoxazine resin and all types of fillers (graphite, graphene,

carbon nanotubes) at an acceleration voltage of 15 kV. The composites and all types of fillers were coated with thin film made of gold using a JEOL ion sputtering device (model JFC-1200) for 4 min to obtain a thickness of approximately 30Å. Then, the micrographs of each specimen fracture surface were taken. The micrographs were used to investigate the dispersion of graphite, graphene, and carbon nanotubes in the polymer matrix thoroughly.

CHAPTER V

RESULTS AND DISCUSSION

5.1 Graphite-filled Polybenzoxazine Characterization

5. 1. 1 Actual Density and Theoretical Density of Graphite Filled Polybenzoxazine Composites

Density of the composite is an important property to confirm the exact amount of filler content and no void formation in the specimen. Figure 5.1 shows theoretical density of graphite filled polybenzoxazine composite which calculated from rule of mixture (equation 4.2) and the actual density which measured by water displacement method (ASTM D792 Method A). The densities of graphite and polybenzoxazine used to calculate theoretical density of the composite are 2.0 and 1.19 g/cm^3, respectively. From the result, the actual densities and the theoretical densities of graphite filled polybenzoxazine composites increased with increasing the graphite content which followed the rule of mixture. The highest maximum packing density of the graphite/ polybenzoxazine filled composite was 84 wt%. Increasing graphite content more than 84 wt% caused an actual density of the composite to be slightly lower than its theoretical density. It might because of the formation of void in the composite. This high maximum packing density occurred because benzoxazine resin which has low melt viscosity could generate strong interaction with large amount of the graphite

which has high average diameter, low aspect ratio, and low specific surface area. This highest maximum packing density was higher than that of graphite-filled phenolic composite of 65%vol [25] and graphite-filled high density polyethylene (HDPE) composite of 50%vol [72].

5. 2 Characterization of Graphite/ Graphene/Carbon Nanotubes Filled Polybenzoxazine Composites

5.2.1 Actual Density and Theoretical Density of Graphite/Graphene/Carbon Nanotubes Filled Polybenzoxazine Composites

Densities of graphite/graphene/carbon nanotubes filled polybenzoxazine composites were measured and compared with their theoretical densities which was calculated using equation 5.1.

$$\rho_c = \frac{1}{\frac{w_{graphite}}{\rho_{graphite}} + \frac{w_{graphene}}{\rho_{graphene}} + \frac{w_{CNTs}}{\rho_{CNTs}} + \frac{w_m}{\rho_m}} \quad (5.1)$$

Where ρ_c = theoretical density of each composite (g/cm^3)

$w_{graphite}$ = weight content of graphite (wt%)

$\rho_{graphite}$ = theoretical density of graphite (= 2.0 g/cm^3)

$w_{graphene}$ = weight content of graphene (wt%)

$\rho_{graphene}$ = theoretical density of graphene (= 2.2 g/cm^3)

w_{CNTs} = weight content of carbon nanotubes (wt%)

ρ_{CNTs} = theoretical density of carbon nanotubes (= 2.0 g/cm^3)

w_m = weight content of matrix (wt%)

ρ_m = density of the matrix (= 1.19 g/cm^3)

The theoretical densities of all specimens were calculated to be about 1.815 g/cm^3. Figure 5.2 illustrates the density of the composite filled with 7.5wt% graphene content and varied carbon nanotubes content at an expense of graphite. The result showed that at 0-2wt% carbon nanotubes, the actual densities of specimens was nearly equal to their theoretical value confirming an exact content of each fillers and no void generation. However, more than 2.5 wt% of carbon nanotubes, a decrease in actual density was observed. It was because the wettability of matrix to wet a greater surface area of carbon nanotubes reduced thus some void or air gap was generated [8]. It is known that the presence of void reduced the properties of the prepared composite [73]. For this reason, the content of carbon nanotubes used in this research were not higher than 2.0wt%.

5. 2. 2 Curing Behavior of Graphite/ Graphene/Carbon Nanotubes Filled Polybenzoxazine Composites

The curing characteristics of the graphite/ graphene/ carbon nanotubes filled benzoxazine compounds were investigated by a differential scanning calorimeter with a temperature range of 30- 300°C and a heating rate of 10°C/ min under nitrogen atmosphere. Figure 5.3 shows thermograms of the compounds having various graphite and carbon nanotubes contents. The thermogram of the neat benzoxazine resin showed an exothermic peak at 233°C due to the oxazine ring opening polymerization.

The thermograms of the compounds having carbon nanotubes contents of 0, 0.5, 1, 1.5 and 2wt% showed exothermic peaks at 224, 223, 222, 222 and 220°C, respectively. An Increasing the carbon nanotubes content caused the exothermic peak to shift to a lower temperature because carbon nanotubes acted as a catalyst to open the oxazine-ring. The catalytic activity of carbon nanotubes confirmed by the FTIR spectrum as shown in figure 5.4. The peaks of the carboxylic (COOH) group were noticed at 1733 and 3444 cm^{-1} of C=O stretching and O-H stretching, respectively. The effect of carboxylic group as a catalyst for ring-opening polymerization of benzoxazine resin was confirmed by P. Kasemsiri *et al.* [74] in the study of cashew nut shell liquid and benzoxazine resin.

Furthermore, the heat of reactions which calculated from area under exothermic peaks decreased with increasing carbon nanotubes contents. The values of the specimen having 0wt% of carbon nanotubes decreased from 46.0 J/g to 25.3 J/g for the specimen having 2wt% of carbon nanotubes. This phenomenon also confirmed that carbon nanotubes acted as a catalyst to cure the compound partially.

Figure 5.5 illustrates thermograms of graphite/graphene/carbon nanotubes benzoxazine compounds having a constant carbon nanotubes content of 0.5wt% and varying curing temperature from 0-3 hours. From this figure, the height and area of exothermic peaks decreased when increasing curing time. A heat of reaction of the uncured compound was determined to be 31.26 J/g. After curing process, heat of reactions decreased to 8.99, 1.81 and 0.68 J/g for the curing times of 1, 2, and 3 hours,

respectively. The degree of conversion of each compound which was calculated by equation 5.2 was 94% after curing for 2 hours. Therefore, the curing condition at the temperature of 200°C for 2 hours was used to cure all specimens for further characterization.

$$\%\text{conversion} = \left(1 - \frac{H_{rxn}}{H_0}\right) \times 100 \quad (5.2)$$

Where H_{rxn} = the heat of reaction of the partially cured specimens.

H_0 = the heat of reaction of the uncured specimens.

5. 2. 3 Dynamic Mechanical Properties of Graphite/ Graphene Filled Polybenzoxazine Composites

Storage modulus (E') and loss modulus (E'') of the specimen were investigated by a dynamic mechanical analyzer with a temperature range of 25-300°C and a heating rate of 5°C/min under nitrogen atmosphere. The storage moduli of the composites were illustrated as shown in Figure 5.6. From the figure, the storage moduli at room temperature of the composites increased with increasing carbon nanotubes content. The graphite/graphene filled polybenzoxazine composite had the storage modulus of 9.6 GPa where the specimen having 0.5, 1, 1.5, and 2wt% of carbon nanotubes at an expense of graphite showed an increase in the storage modulus to 9.7, 10.0, 10.3, and 11.4 GPa which accounted to be 17.5% higher than that of the graphite/graphene filled polybenzoxazine (5.2 GPa) and also higher than that of graphite-filled HDPE composite developed by A. Pandey *et al*. [72]. This phenomenon occurred because carbon

nanotubes which have high rigidity generated substantial adhesion between the matrix and the other fillers and improved stiffness of the composites. Moreover, the moduli at the rubbery plateau region of the composites were also increased with increasing carbon nanotubes content. This phenomenon confirmed that the substantial interaction between the matrix and all types of fillers were occurred. However, the moduli were slightly less than that of graphite/graphene filled polybenzoxazine composite developed by M.Phuangngamphan [29]. It might because a lower surface area of greater size of graphite size used in this research caused a less substantial interaction to benzoxazine matrix compared to that of having higher surface area [75].

Loss moduli of all specimens were illustrated in Figure 5.7. The temperature at the peak of loss modulus of each specimen was used as glass transition temperature (T_g) of its sample. The T_g values of the composites increased when increasing carbon nanotubes content. T_g values of graphite/graphene polybenzoxazine composite were 198°C. At 0.5, 1, 1.5, and 2wt% carbon nanotubes content, the values of the specimens increased to 201, 203, 203, and 207°C, respectively. This high T_g values was 9°C higher than that of the graphite/graphene filled polybenzoxazine and also higher than that of graphite-filled polybenzoxazine composite developed by I. Dueramae *et al*. [21] This phenomenon implied the strong interaction between carbon nanotubes and polybenzoxazine. These types of fillers impeded mobility of the polymer chain, reduced free volume and raised crosslink density. However, T_g values of our system were slightly less than that of graphite/graphene filled polybenzoxazine composite

which attributed to that the polymer chain can moves easily compared to that having a small graphite size [75, 76].

5.2.4 Thermal Stability of Graphite/ Graphene/ Carbon Nanotubes Filled Polybenzoxazine Composite

Figure 5.8 shows thermal stability of graphite/graphene/carbon nanotubes filled polybenzoxazine composites obtained from a thermogravimetric analyzer with a temperature range of 25- 850°C and a heating rate of 20°C/ min under nitrogen atmosphere. From Figure 5.8, the temperature at 5% weight loss of each specimen is used as its thermal degradation temperature. From the result, the degradation temperature of neat polybenzoxazine was 334°C. Graphite had extremely high thermal stability so it did not degrade in this temperature range while graphene and carbon nanotubes had a little degradation due to degradation of oxygen-containing functional groups which confirmed by FTIR spectra. These functional groups in graphene and carbon nanotubes could help to improve mechanical properties of the composites by generate good interfacial bonding with the matrix. Increasing carbon nanotubes contents made enhancement of thermal degradation temperature attribute to high stability carbon nanotubes acted as gas barrier to prevent degradation of volatile products. The thermal degradation temperatures of the composites having 0-2 wt% carbon nanotubes were found to be 422, 423, 428, 442, and 466 °C, respectively.

Moreover, thermal degradation temperatures of graphite/graphene carbon nanotubes filled polybenzoxazine composite in this research were higher than those

of graphite/graphene filled polybenzoxazine composite as studied by M. Phuangngamphan having the value of 433°C [29]. This extremely high thermal stability was attributed to that carbon nanotubes which have higher specific surface area than graphite could restrict mobility of the polymer matrix [65] and also generated labyrinth to delay diffusion of volatile products [77]. It was also found that carbon nanotubes filled polybenzoxazine composite had higher thermal degradation temperature than that of graphite filled polybenzoxazine composite or graphene filled polybenzoxazine composite at same filler content [7, 21, 78].

Char residue at 800°C of the neat polybenzoxazine was about 26.0%. Graphite had 100% char residue while graphene and carbon nanotubes had char residue of 89.7% and 96.8%, respectively, due to degradation of volatile functional groups such as carboxylic group which confirmed by their FTIR spectra. Decreasing graphite content and increasing carbon nanotubes content decreased char residue of the specimen. Char yields were found to be 93.3, 90.9, 90.6, 90.2, and 89.9% of the composites with 0-2 wt% respectively. This phenomenon was appropriated to higher thermal stability of graphite which had no other volatile functional groups.

5.2.5 Specific Heat Capacity of Graphite/ Graphene/ Carbon Nanotubes Filled Polybenzoxazine Composite

Specific heat capacity was defined from the amount of energy absorbed by a unit mass of material to raise a unit of temperature in constant pressure. This

parameter was used along with thermal diffusivity to calculated thermal conductivity from equation 4.4 [79].

$$k = \rho \times c_p \times \alpha \quad (4.4)$$

Specific heat capacity of the specimen was investigated by a differential scanning calorimeter. Figure 5.9 illustrates specific heat capacity of the composite having various carbon nanotubes content. From the results, specific heat capacity of each specimen which measured from DSC was not different significantly with increasing carbon nanotubes content at an expense of graphite because both carbon nanotubes and graphite have similar specific heat capacity. Furthermore, this result showed that specific heat capacity of the composites was the structure-intensitive property which had linear relationship with filler contents. In addition, specific heat capacity was the property which follow rule of mixture as shown in equation 5.3

$$c_{pc} = c_{p,graphite} w_{graphite} + c_{p,graphene} w_{graphene} + c_{p,CNT} w_{CNT} + c_{pp} w_p \quad (5.3)$$

Where c_{pc} and c_{pp} are specific heat capacity of composite and neat polybenzoxazine respectively. While w_p is mass fraction of neat polybenzoxazine in the composite.

Specific heat capacity of graphite, graphene, carbon nanotubes and polybenzoxazine were 0.770, 1.075, 0.770 and 1.756 J/g·K, respectively. Specific heat capacity of the composites were calculated to be 0.951 J/g·K for all specimens from rule of mixture as shown in table 5.1. The result show that specific heat capacity of all

composites was close to 0.951 J/g·K (0.984, 0.990, 0.953, 0.946, and 0.965 J/g·K for composites with 0.0, 0.5, 1.0, 1.5, and 2.0 wt% of carbon nanotubes, respectively).

5.2.6 Thermal Diffusivity of Graphite/Graphene/Carbon Nanotubes Filled Polybenzoxazine Composite

Thermal diffusivity is one property used to calculate thermal conductivity using equation 4.4. It is commonly conducted by laser flash method in which the heat propagates from top to bottom of the specimen. Thermal diffusivities at 25°C of the composites with varying carbon nanotubes content were shown in Figure 5.10. From the figure, thermal diffusivities of the samples increased with increasing carbon nanotubes content. At 0.0, 0.5, 1.0, 1.5, and 2.0wt% carbon nanotubes, thermal diffusivities at room temperature were measured to be 8.213, 11.836, 11.948, 12.060, and 12.115 mm^2/s, respectively. This phenomenon occurred because of the presence of highly thermally conductive carbon nanotubes.

For non-metal materials such as carbon-filled composites, heat transports by flow of phonons or lattice vibrational energy. Phonons normally flow through a material through the speed of sound. However, phonon scattering is sometimes occurred to delay flow of phonons and increase heat resistance in a material. This phenomena depends on temperature [17, 80, 81].

Figure 5.11 illustrates thermal diffusivities of the composites at temperature ranging from 25-180°C. The results showed that the diffusivities of all specimens were decreased with increasing temperature because higher temperature caused more

phonon-phonon scattering process and increase thermal resistivity of the composite [80, 81]. In addition, the composites filled with higher carbon nanotubes content had a higher slope than that of the composites with a lower filler content implied that a more temperature sensitivity of the composites with increasing carbon nanotubes content.

5.2.7 Thermal Conductivity of Graphite/ Graphene/ Carbon Nanotubes Filled Polybenzoxazine Composite

To achieve high thermal conductivity of non- metal material i.e. polymer composite, higher content of conductive filler is necessary to generate conductive network and minimize heat resistance occurred by three phenomena (phonon-phonon scattering, boundary scattering, and defect scattering) [17, 60, 80, 81].

Thermal conductivity of the composites can be calculated using equation 4.4 where density, specific heat capacity, and thermal diffusivity of each specimen were determined. Thermal conductivities of each specimen were summarized in Table 5.2.

Figure 5.12 displays through-plane thermal conductivity of the composite having various carbon nanotubes content. Thermal conductivity of the neat polybenzoxazine was 0.274 W/m·K. The presence of graphite and graphene in the composite promoted thermal pathway so that thermal conductivity increased to 14.7 W/m·K. The high conductivity was attributed to that graphite with large average diameter was able to fill in the composite in a high content and generated good conductive pathway with low phonon-phonon scattering and low boundary scattering

and graphene which have high aspect ratio can form conductive path between graphite gap. An addition of carbon nanotubes content also increased thermal conductivity of the samples. The thermal conductivties of the specimens having 0.5, 1.0, 1.5, and 2.0wt% carbon nanotubes were calculated to be 21.3, 20.6, 20.7 and 21.3 W/m·K, respectively. The highest thermal conductivity value of graphite/ graphene/ carbon nanotubes filled polybenzoxazine composite was 21.3 W/m·K or about 44 times greater than that of the composite without carbon nanotubes. This very high thermal conductivity was obtained because carbon nanotubes having such high aspect ratio (long length and small diameter) oriented randomly which improve thermal conductivities in three directions [25]. Moreover, carbon nanotubes can contact with adjacent graphene and graphite by bridge between two particles to form conductive network effectively [65]. These phenomenon can increase transfer efficiency of phonon through the specimen. The highest thermal conductivity was higher than that of graphite filled polybenzoxazine composite developed by I. Dueramae *et al.* (10.2 W/m·K) [21], graphene filled polybenzoxazine composite developed by R. Plengudomkit *et al.* (8.03 W/m·K) [7], graphite/carbon nanotubes filled phenolic composite developed by S.R. Dhakate *et al.* (13 W/m·K) [25] and graphite/ graphene filled polybenzoxazine composite developed by M.Phuangngamphan (14.5 W/m·K) [29]. Moreover, the composites filled with carbon nanotubes have higher conductivities than the requirement of DOE in 2020 (more than 20 W/m·K).

However, this study examined through-plane thermal conductivity of the composite because it is a key property to transport heat out of the cells. Through-plane thermal conductvitiy is normally much lower than the in-plane value due to anisotropic structure of the filler as studied by X. Tian *et al.* [62].

5.2.8 Electrical Conductivity of Graphite/ Graphene/ Carbon Nanotubes Filled Polybenzoxazine Composite

During the operation of proton exchange membrane fuel cells, electrons transfer from anode through two bipolar plates to cathode in order to complete the circuit. Electrical conductivity of bipolar plates is the key property to minimize number of plates along with reduce weight and cost [82]. To obtain high electrical conductivity in polymer composite, the conductive particles must contact to each other as much as possible to generate a continuous conductive pathway for electron to flow through independently [13].

There are two types of electrical conductivity i.e. through-plane and in-plane. The in-plane conductivity is more important property than the through-plane due to the larger area. Figure 5.12 shows in-plane electrical conductivity of the composite by varying carbon nanotubes content. It was found that an increase of carbon nanotubes in the composites resulted in an increase in electrical conductivity. The electrical conductivities of the composite having 0.0, 0.5, 1.0, 1.5, and 2.0wt% were measured to be 320, 333, 340, 360, and 364 S/cm, respectively. The improvement of this property was attributed to a high aspect ratio of carbon nanotubes which generated conductive

pathway easily [8, 66, 83]. These types of fillers could overlap and interlace easily and also generated electrical conductive pathway with adjacent graphite and graphene [65, 84]. This phenomenon was also found by S.R. Dhakate *et al.* in graphite/carbon nanotubes phenolic composite [25] and J. Che *et al.* in graphite/carbon nanotubes HDPE composite [66]. The highest in-plane electrical conductivity was found to be 364 S/cm in the composite with 2.0wt% filler content which higher than that of graphite/graphene polybenzoxazine composite developed by M.Phuangngamphan [29] in which the value meet DOE target as it is required to be higher than >100 S/cm) [11-14].

5.2.9 Flexural Properties of Graphite/Graphene/Carbon Nanotubes Filled Polybenzoxazine Composite

Bipolar plates have a duty to protect the membrane and electrodes from external force. Flexural strength and modulus of the composite with different carbon nanotubes loading is illustrated by figure 5.13 and 5.14 respectively. From the figure 5.13, flexural strength, increasing carbon nanotubes content along with decreasing graphite content can slightly enhance flexural strength. For the composite having 0, 0.5, 1, 1.5, and 2 wt% carbon nanotubes content, the strength was reported to be 28.1, 34.2, 33.7, 39.4, and 41.5 MPa, respectively or about 41% improvement. This improving of flexural strength occurred because multi-walled carbon nanotubes have higher intrinsic mechanical properties than graphite. The load applied to the composite could transfer to carbon nanotubes efficiency because of high aspect ratio of carbon

nanotubes [85]. Moreover, their tube-like shape caused well-dispersed in polymer matrix and their structure with have kinks and twists can prevent detachment of these fillers from matrix [67]. This phenomenon also occurred in graphite/carbon nanotubes filled phenolic resin investigated by S.R.Dhakate *et al.* [25]. The flexural strengths of the composites were still greater than that required by DOEs (>25 MPa) [11-14].

From the result, flexural modulus was improved with increasing carbon nanotubes content in the composite. The flexural moduli of the composites with 0, 0.5, 1, 1.5, and 2 wt% carbon nanotubes content were investigated to be 20.9, 36.5, 34.7, 37.7, and 49.7 GPa, respectively or about 93% improvement. This enhancement was attributed to the carbon nanotubes which dispersed easily and generated substantial bonding with matrix and other fillers, retard movement of the polymer chain, and also increase crosslink ratio. Furthermore, carbon nanotubes have the highest aspect ratio of all types of fillers. These high aspect ratio cause more improvement of the modulus than graphite or graphene [67]. For this reason, the stiffness of the composites was improved. The flexural moduli were higher than those of graphite/graphene filled polybenzoxazine composite developed by M.Phuangngamphan [29] which found to be 16.8 GPa and also greater than values required by DOEs (>10 GPa) [11-14].

5.2.10 Water Absorption of Graphite/Graphene/Carbon Nanotubes Filled Polybenzoxazine Composite

In the operation of fuel cells, water is generated from the electrochemical reactions and flow through bipolar plates. For this reason, water absorption or water uptake of the bipolar plates must be as low as possible to prevent damage within fuel cells. Water absorption can be calculated using equation 4.9

$$\% \text{ Water absorption} = \left(\frac{W-W_d}{W_d}\right) \times 100 \quad (4.9)$$

Figure 5.16 illustrates the relation between water absorption of the composite having different carbon nanotubes loading and immersion time from 0-168 hours or 0-7 days. From the figure 5.16, the absorption curves of all specimens rapidly increased within 24 hours. After immersed for 24 hours, the curves slightly increased until the end of experiment. The results showed that percentage of water absorption of the specimens increased with increasing carbon nanotubes content. The higher rate of absorption was attributed to the presence of hydrophilic functional groups such as carboxylic group of nanotube surface which confirmed by FTIR spectra of carbon nanotubes in figure 5.4. This phenomenon also occurred in carbon nanotubes reinforced epoxy/glass fiber laminated developed by N.M.Zulfil *et al.* [86]. However, the water absorption after immersed for 24 hours of all composites filled with carbon nanotubes were calculated to be 0.023-0.114% which was still lower than DOEs target (<0. 3%) [11-14].

5.2.11 SEM Characterization of Graphite/Graphene/Carbon Nanotubes Filled Polybenzoxazine Composite

Figure 5.17 (a) illustrates fracture surface of the neat polybenzoxazine showing a smooth surface. Figure 5.17 (b) to Figure 5.17 (d) reveal micrographs of graphite which large multiple layer of flake-like shape, graphene with stacks of flake-like shape, and carbon nanotubes with large amount of tubes entangle together respectively. Figure 5.17 (e) to figure 5.17 (g) show fracture surfaces of polybenzoxazine composite filled with graphite, graphene, and carbon nanotubes, respectively indicating a well-dispersed of each filler in polymer matrix. Figure 5.17 (h) illustrates the fracture surfaces of the composite filled with 0.5 wt% graphite, graphene and carbon nanotube where Figure 5.17 (i) shows those of the composite filled with 74.5, 7.5 and 2 wt% of graphite, graphene and carbon nanotubes, respectively. The figures reveal well-dispersion of all fillers in polymer matrix attributing to a very low-melt viscosity of benzoxazine resin which provided good wettability to all types of fillers. For highly-filled polybenzoxazine composite, the substantial adhesion between the fillers and the matrix were generated. In addition, each filler occurred to improve the properties of the composite such as thermal conductivity, electrical conductivity, and flexural properties.

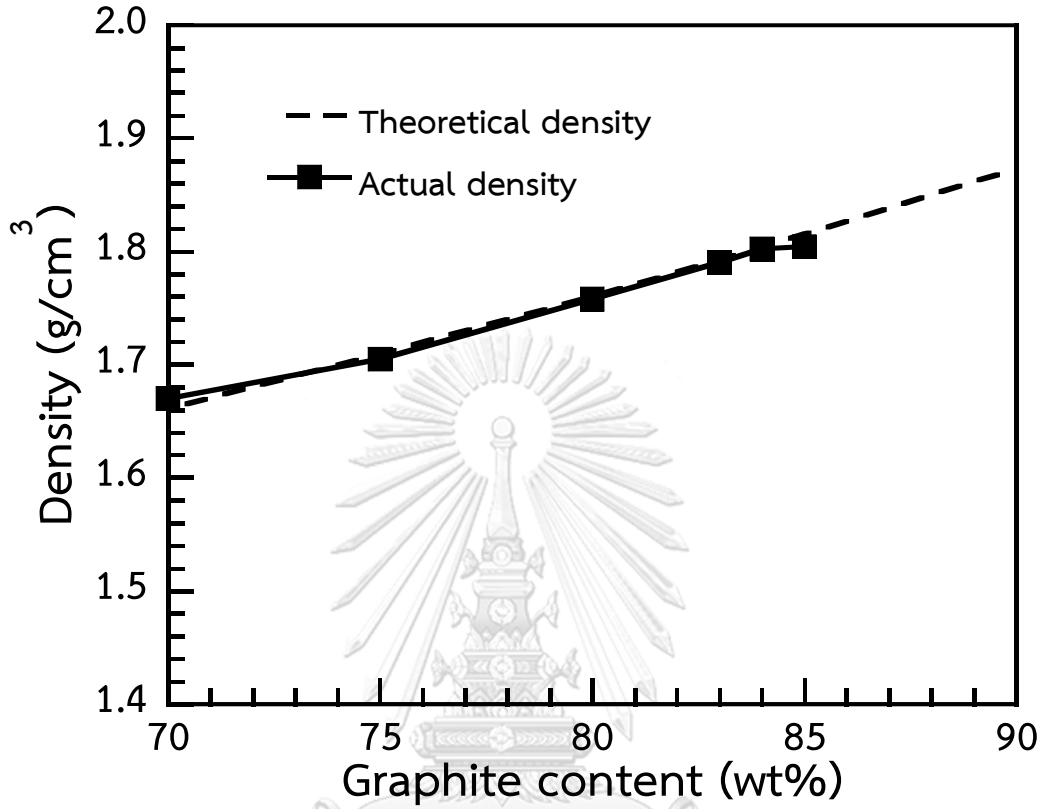

Figure 5.1 Theoretical and actual densities of graphite-filled polybenzoxazine composites with varying graphite content.

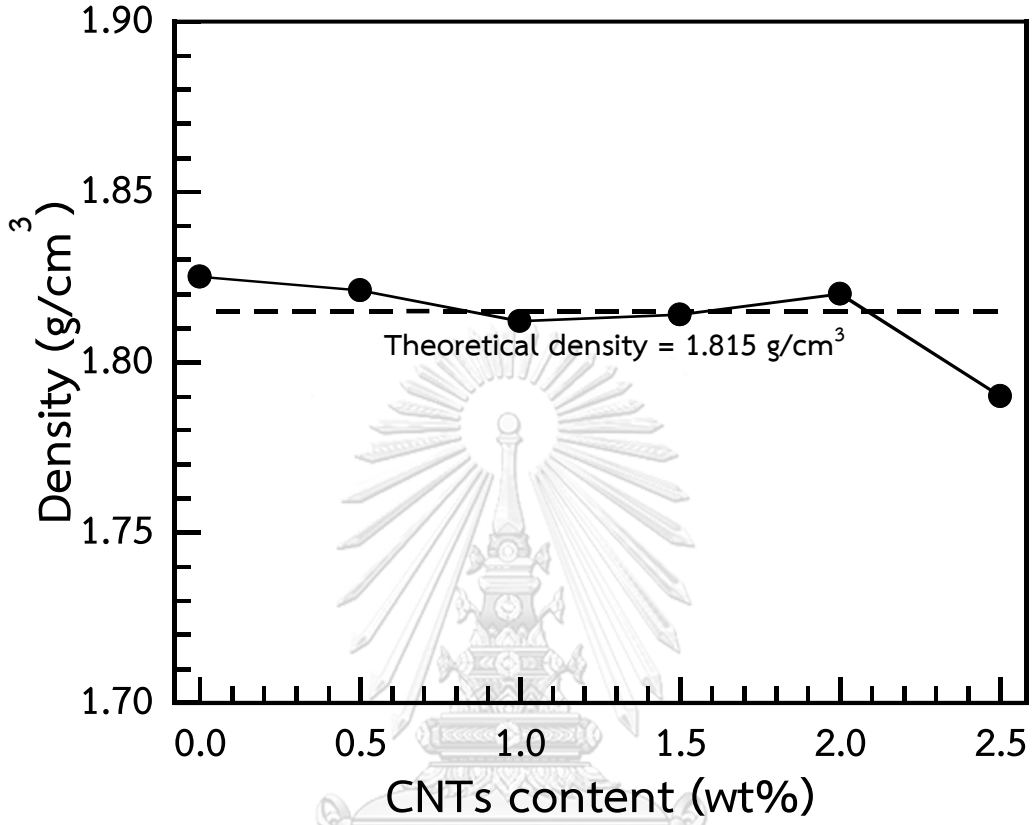

Figure 5.2 Densities of graphite/graphene/carbon nanotubes filled polybenzoxazine composites with varying carbon nanotubes content.

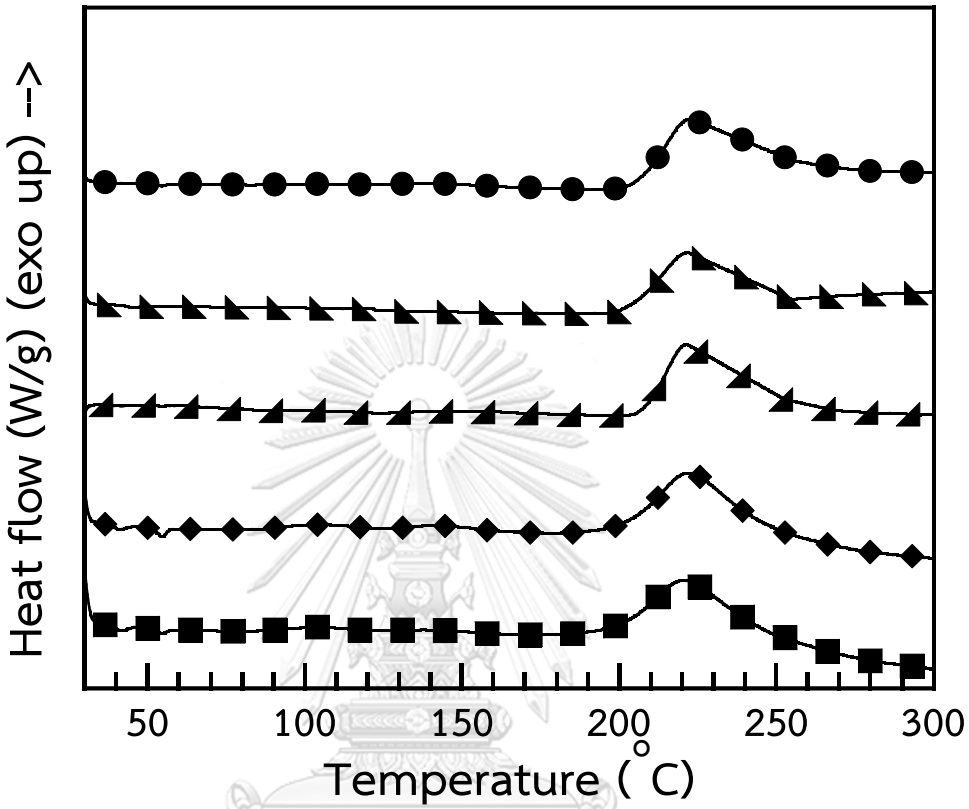

Figure 5.3 DSC thermograms of graphite/graphene/carbon nanotubes filled benzoxazine molding compound with varying carbon nanotubes content: (●) 0.0 wt% carbon nanotubes, (◣) 0.5wt% carbon nanotubes, (◢) 1.0wt% carbon nanotubes, (◆) 1.5wt% carbon nanotubes, (■) 2.0wt% carbon nanotubes.

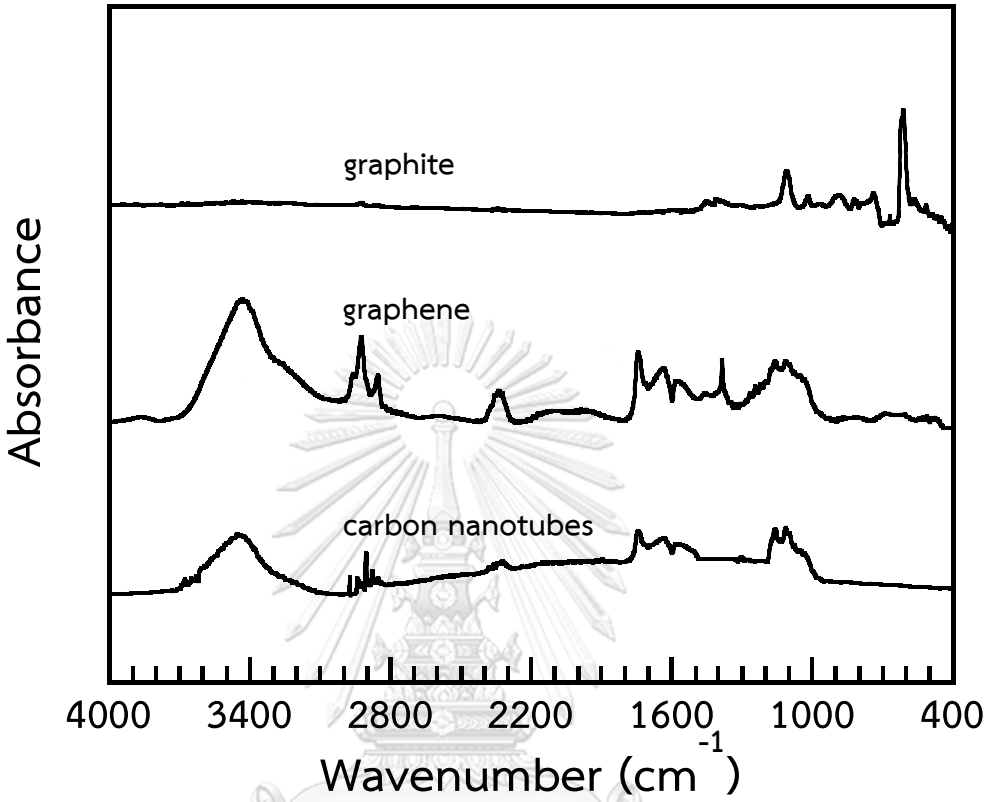

Figure 5.4 FTIR spectra of graphite, graphene, and carbon nanotubes.

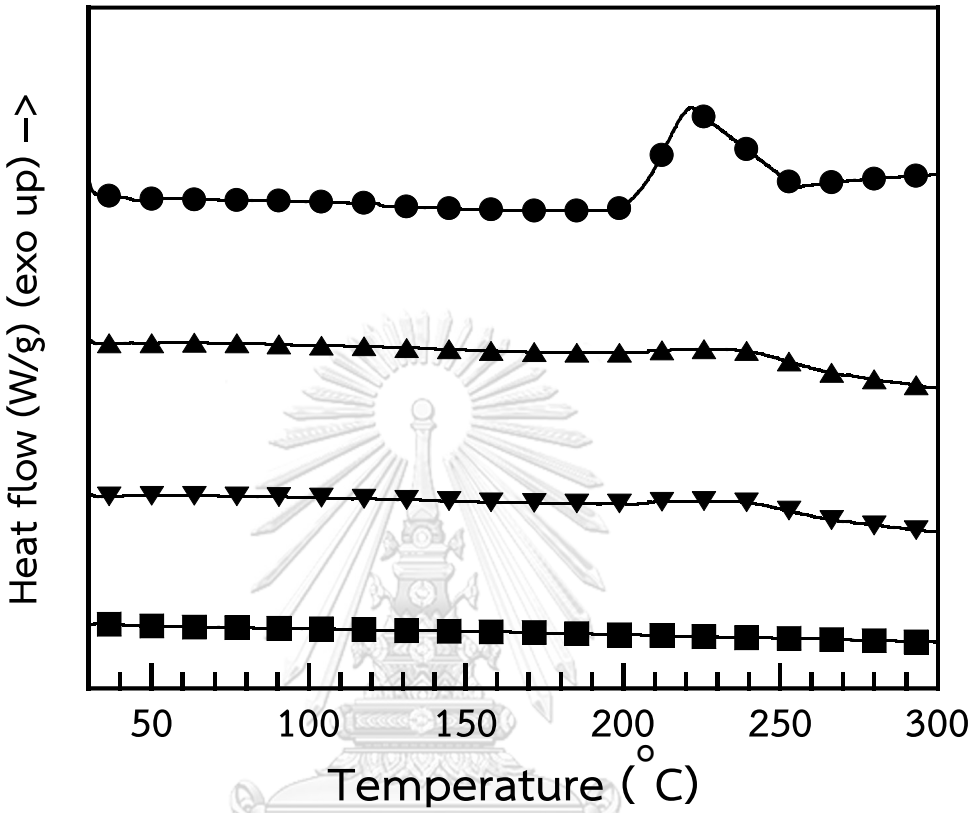

Figure 5.5 DSC thermograms of graphite/graphene/carbon nanotubes filled benzoxazine molding compound: (●) uncured compound, (▲) 1 hour curing, (▼) 2 hours curing, (■) 3 hours curing.

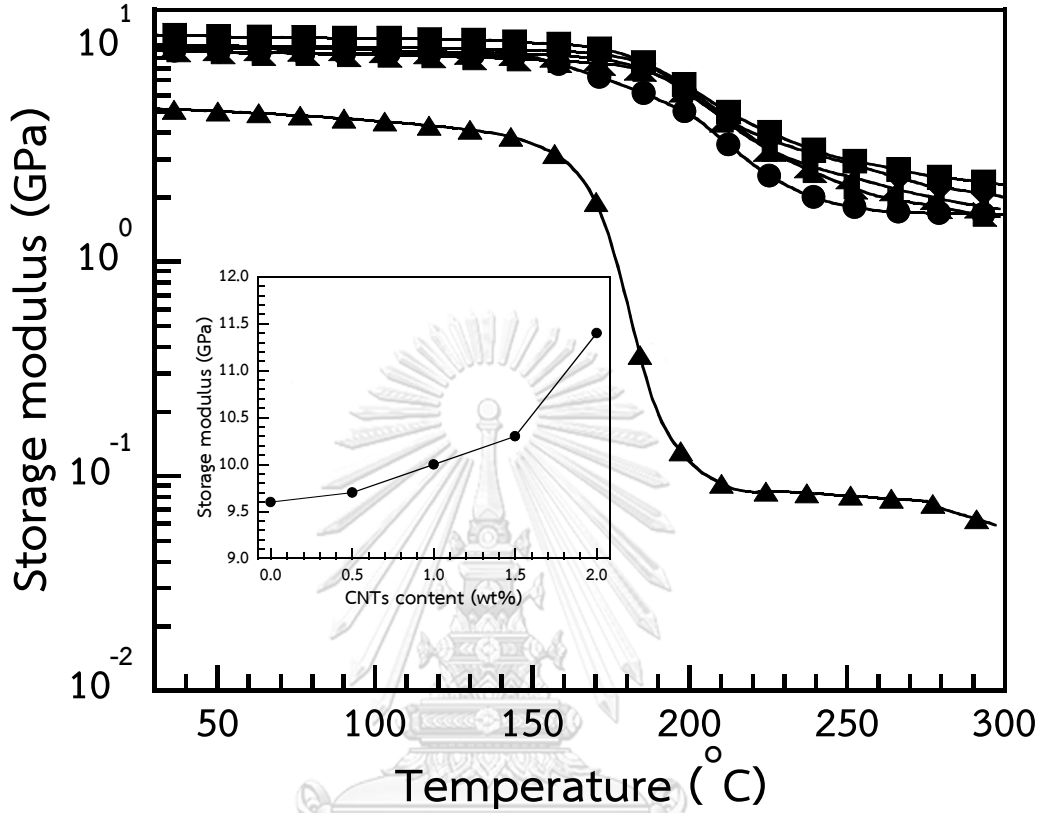

Figure 5.6 Storage moduli of graphite/graphene/carbon nanotubes filled polybenzoxazine composites with varying carbon nanotubes contents: (▲) neat polybenzoxazine, (●) 0.0wt% carbon nanotubes, (◢) 0.5wt% carbon nanotubes, (◣) 1.0wt% carbon nanotubes, (◆) 1.5wt% carbon nanotubes, (■) 2.0wt% carbon nanotubes.

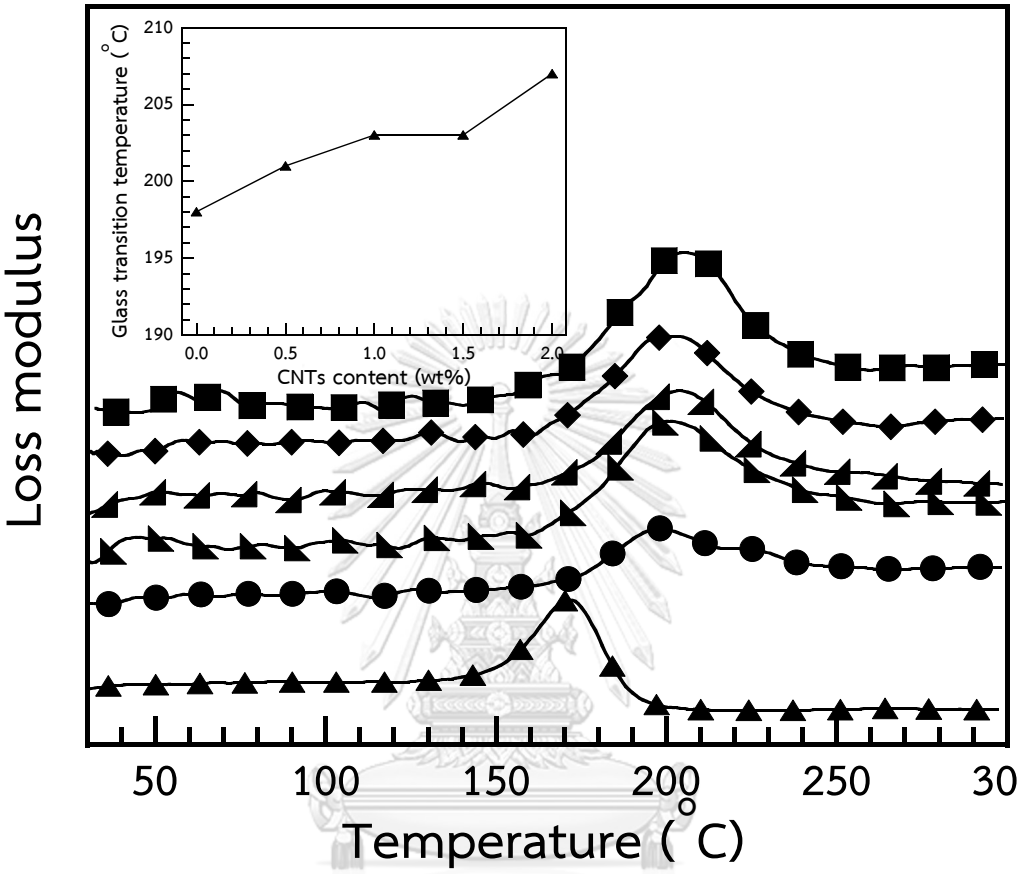

Figure 5.7 Loss moduli of graphite/graphene/carbon nanotubes filled polybenzoxazine composites with varying carbon nanotubes contents: (▲) neat polybenzoxazine, (●) 0.0wt% carbon nanotubes, (◣) 0.5wt% carbon nanotubes, (◢) 1.0wt% carbon nanotubes, (◆) 1.5wt% carbon nanotubes, (■) 2.0wt% carbon nanotubes.

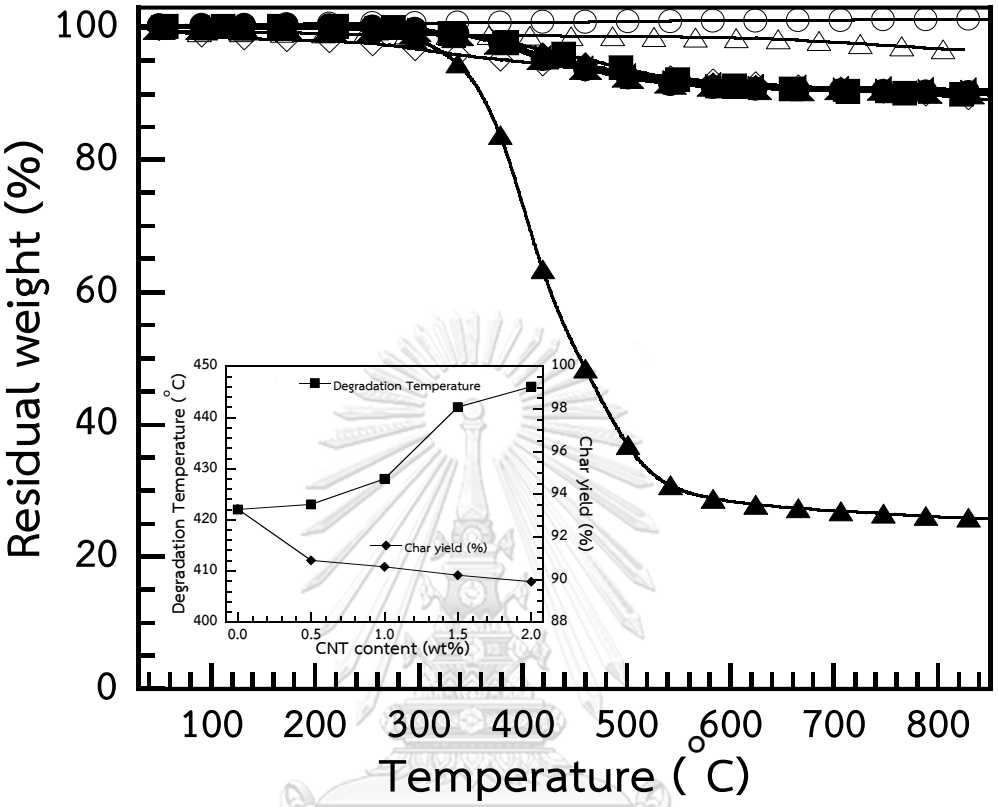

Figure 5.8 Thermal stability of graphite/graphene/carbon nanotubes filled polybenzoxazine composites with varying carbon nanotubes contents: (▲) neat polybenzoxazine, (●) 0.0wt% carbon nanotubes, (◣) 0.5wt% carbon nanotubes, (◢) 1.0wt% carbon nanotubes, (◆) 1.5wt% carbon nanotubes, (■) 2.0wt% carbon nanotubes, (○) graphite, (◇) graphene, (△) carbon nanotubes.

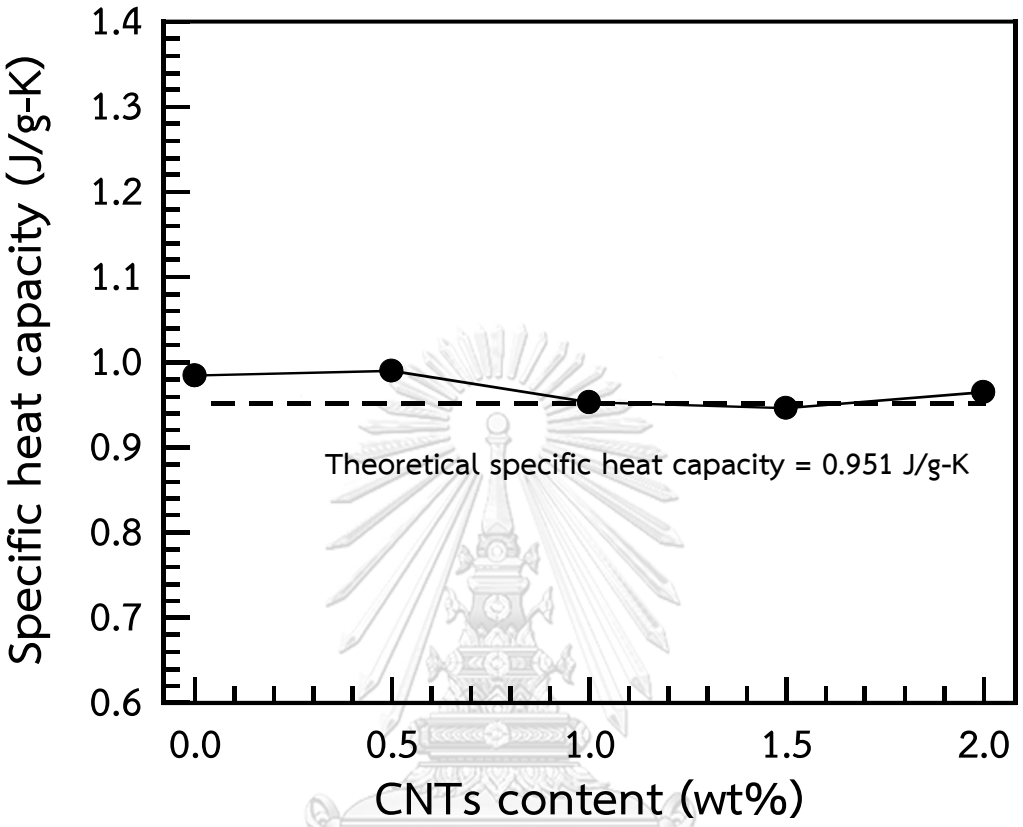

Figure 5.9 Specific heat capacities of graphite/graphene/carbon nanotubes filled polybenzoxazine composites with varying carbon nanotubes contents.

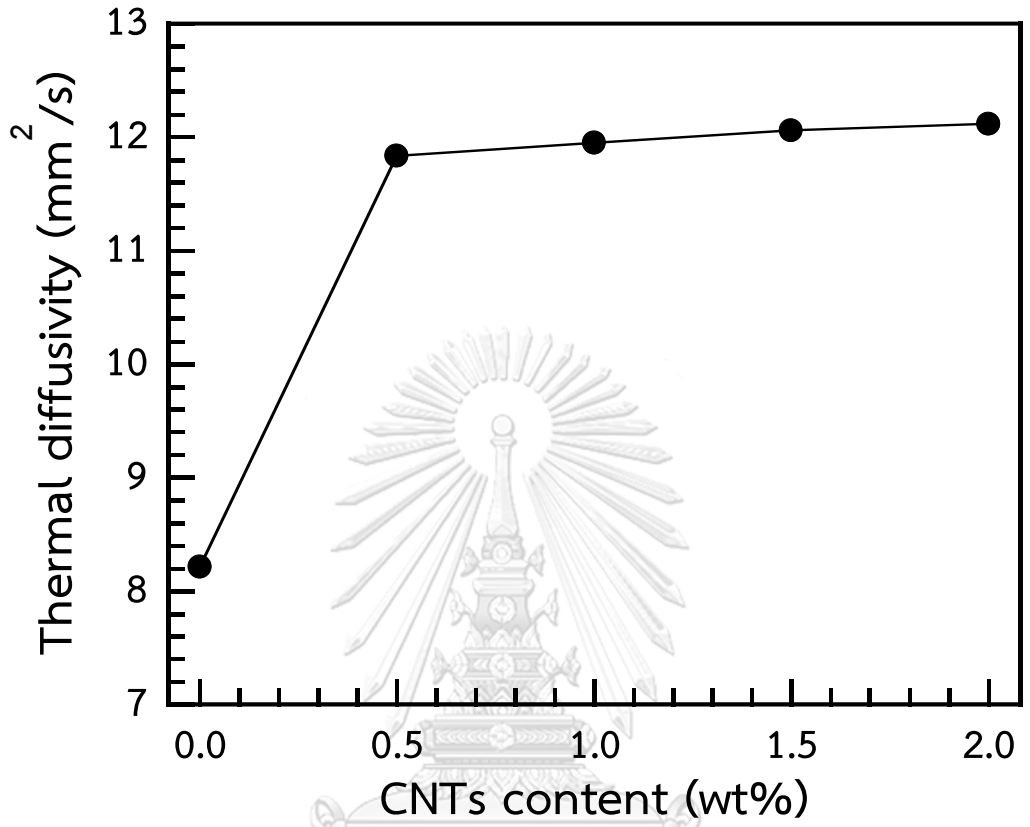

Figure 5.10 Thermal diffusivities at 25°C of graphite/graphene/carbon nanotubes filled polybenzoxazine composites with varying carbon nanotubes contents.

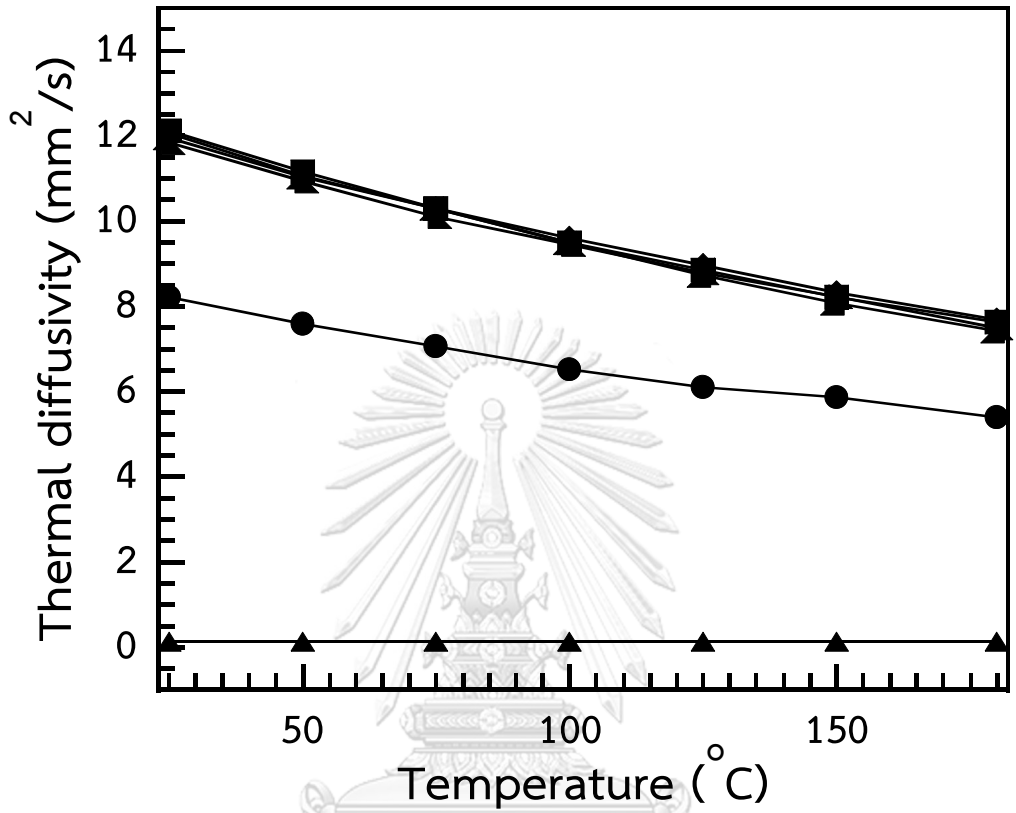

Figure 5.11 Thermal diffusivities of graphite/graphene/carbon nanotubes filled polybenzoxazine composites at various temperature: (▲) neat polybenzoxazine, (●) 0.0wt% carbon nanotubes, (◣) 0.5wt% carbon nanotubes, (◢) 1.0wt% carbon nanotubes, (◆) 1.5wt% carbon nanotubes, (■) 2.0wt% carbon nanotubes.

Table 5.1 Thermal conductivities of graphite/graphene/carbon nanotubes filled polybenzoxazine composites at 25°C.

Filler content (wt%)			ρ	c_p	α	K
Graphite	Graphene	CNTs	(g/cm^3)	(J/g·K)	(mm^2/s)	(W/m·K)
0.0	0.0	0.0	1.190	1.756	0.131	0.274
76.5	7.5	0.0	1.825	0.984	8.213	14.7
76.0	7.5	0.5	1.821	0.990	11.836	21.3
75.5	7.5	1.0	1.812	0.953	11.948	20.6
75.0	7.5	1.5	1.814	0.946	12.060	20.7
74.5	7.5	2.0	1.820	0.965	12.115	21.3

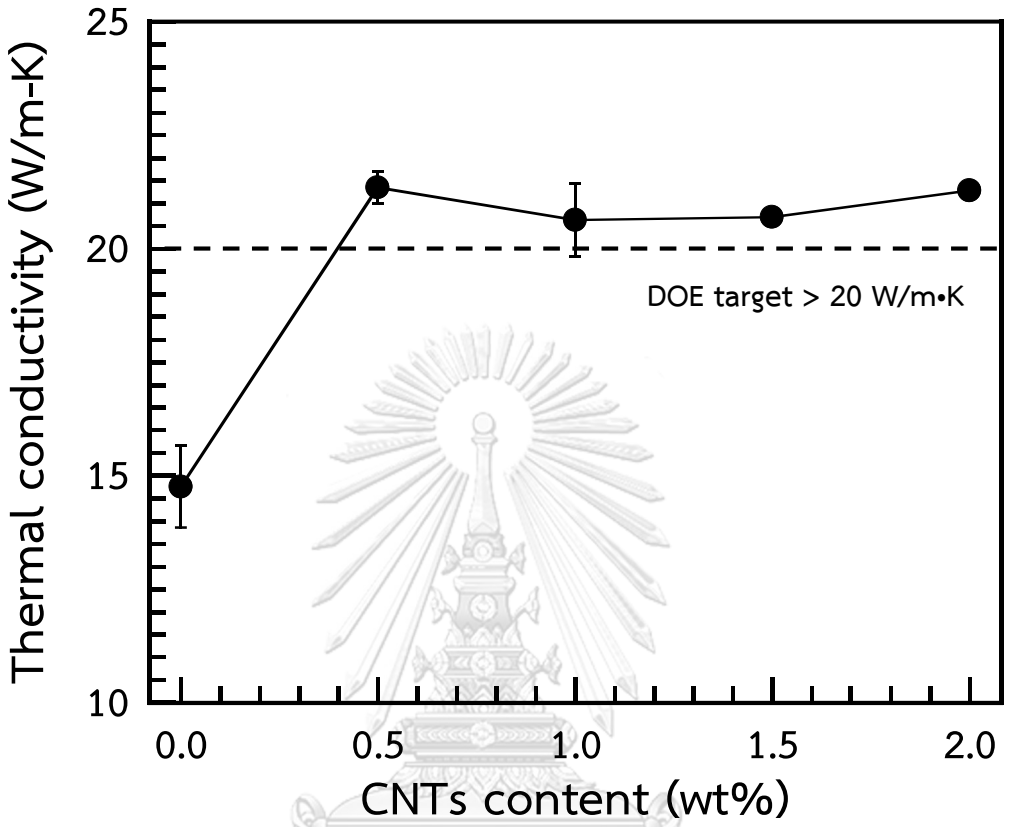

Figure 5.12 Thermal conductivities of graphite/graphene/carbon nanotubes filled polybenzoxazine composites at 25°C.

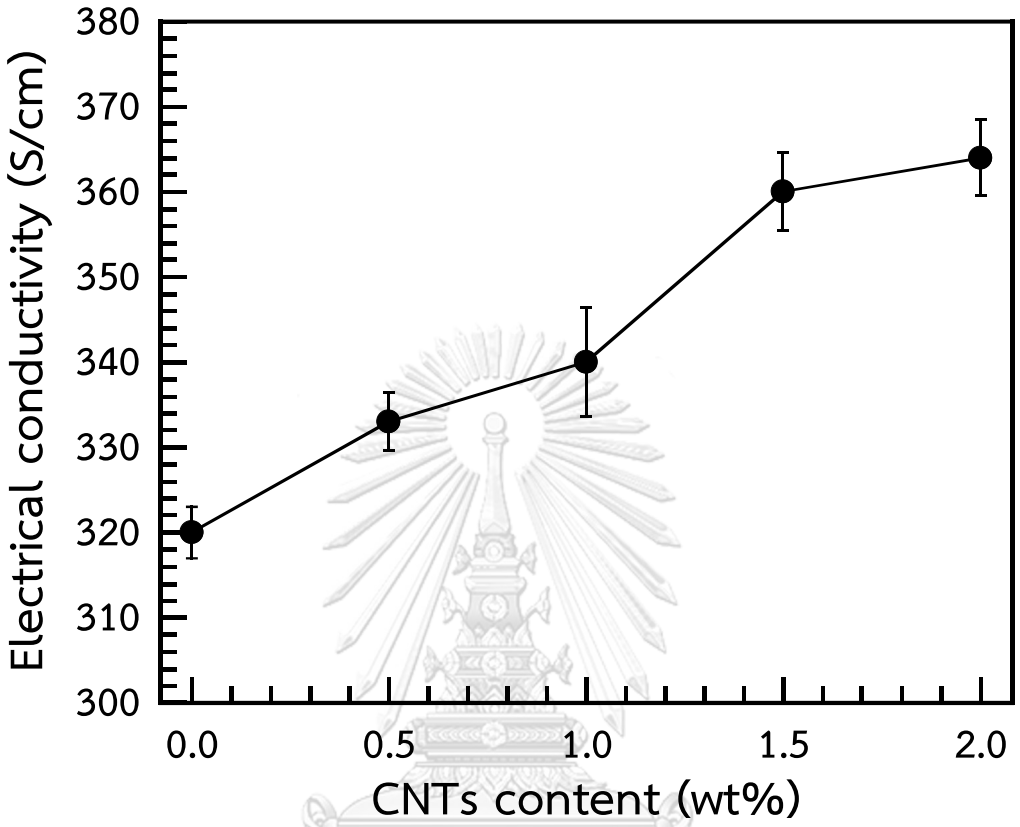

Figure 5.13 Electrical conductivities of graphite/graphene/carbon nanotubes filled polybenzoxazine composite at 25°C.

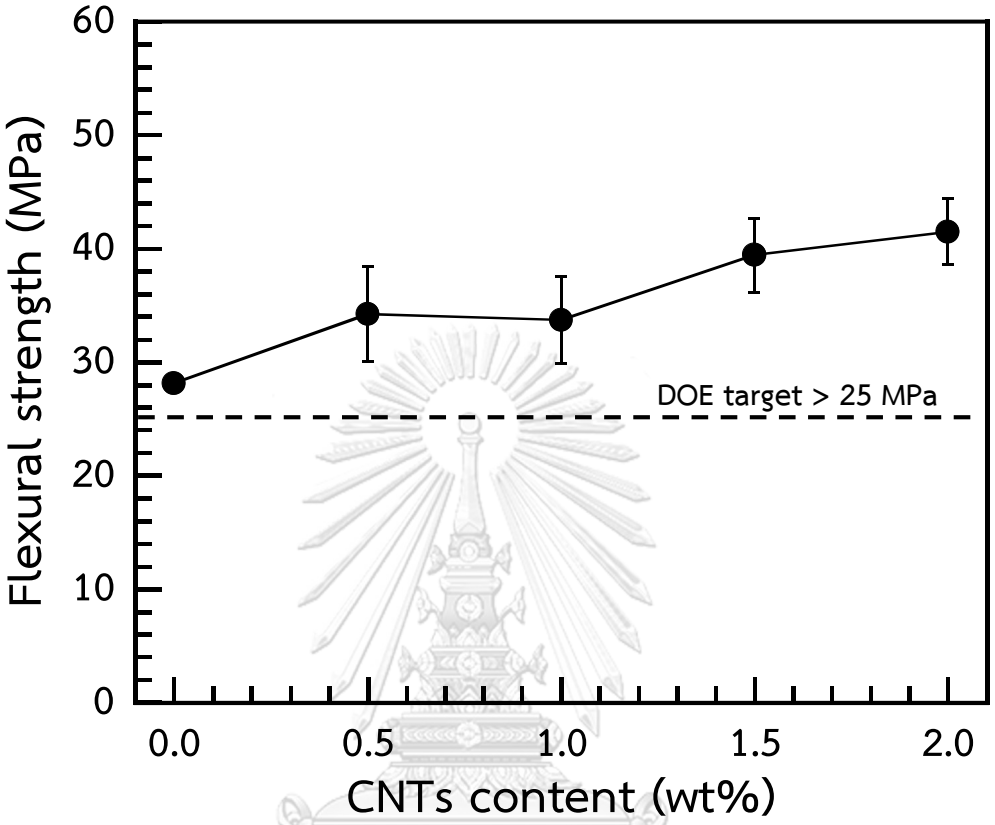

Figure 5.14 Flexural strengths of graphite/graphene/carbon nanotubes filled polybenzoxazine composites with varying carbon nanotubes contents.

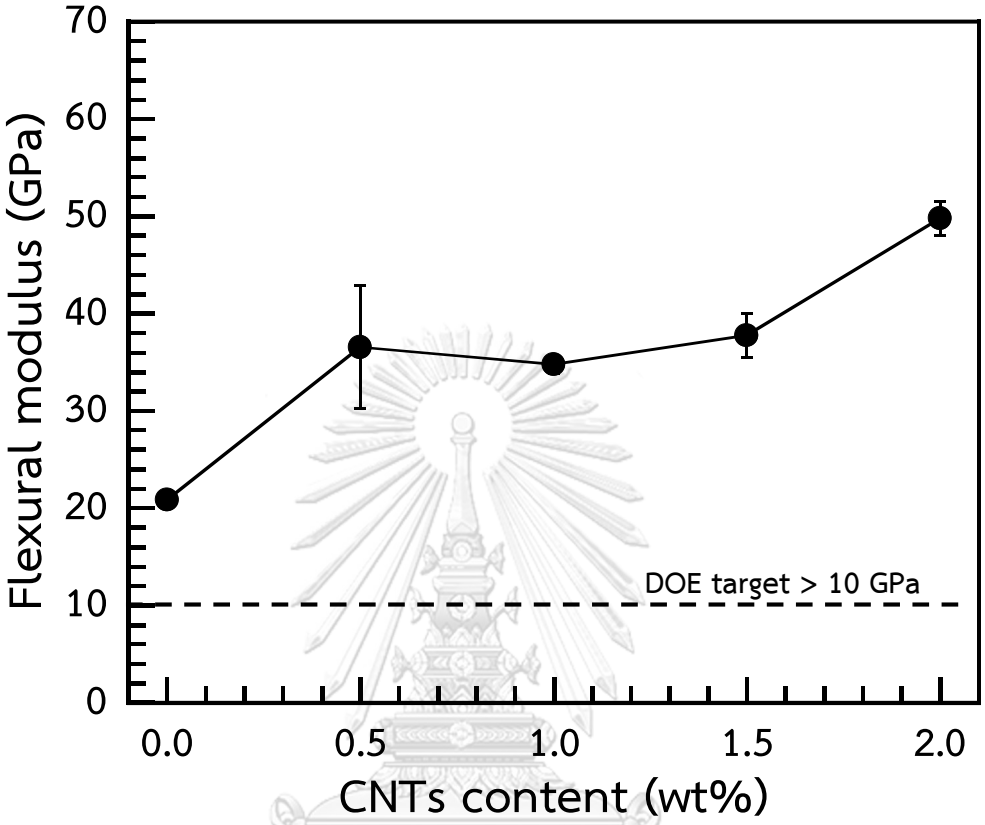

Figure 5.15 Flexural moduli of graphite/graphene/carbon nanotubes filled polybenzoxazine composites with varying carbon nanotubes contents.

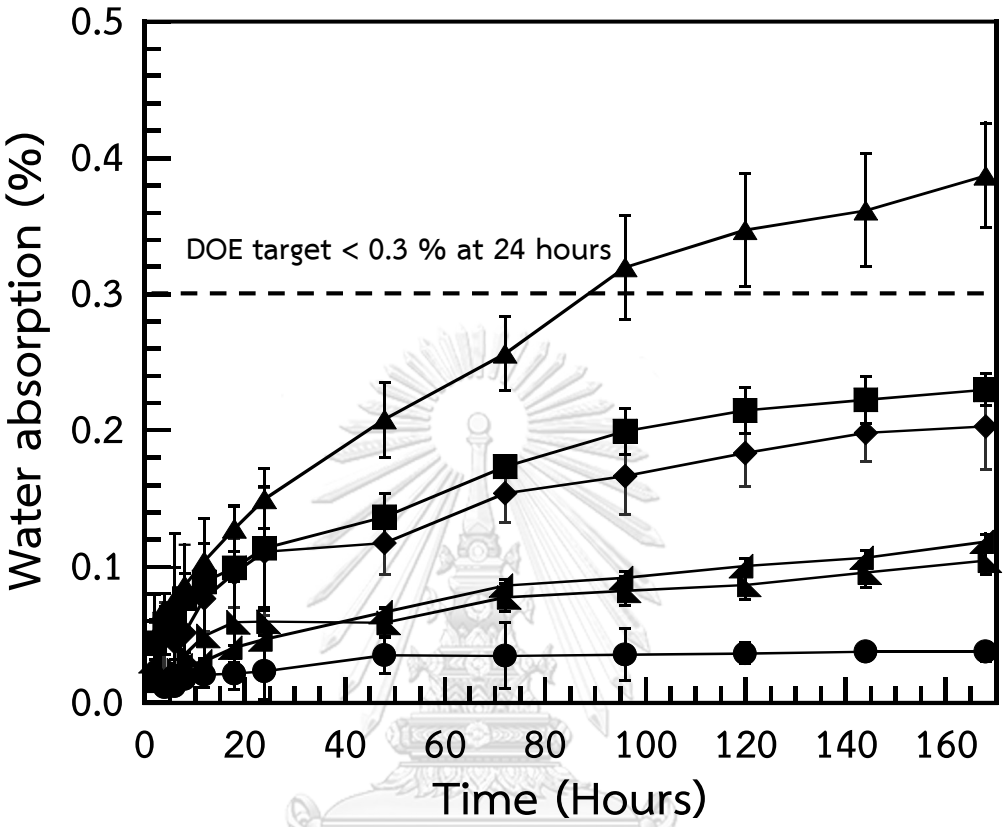

Figure 5.16 Water absorption of graphite/graphene/carbon nanotubes filled polybenzoxazine composites with varying carbon nanotubes contents. (▲) neat polybenzoxazine, (●) 0.0wt% carbon nanotubes, (◣) 0.5wt% carbon nanotubes, (◢) 1.0wt% carbon nanotubes, (◆) 1.5wt% carbon nanotubes, (■) 2.0wt% carbon nanotubes.

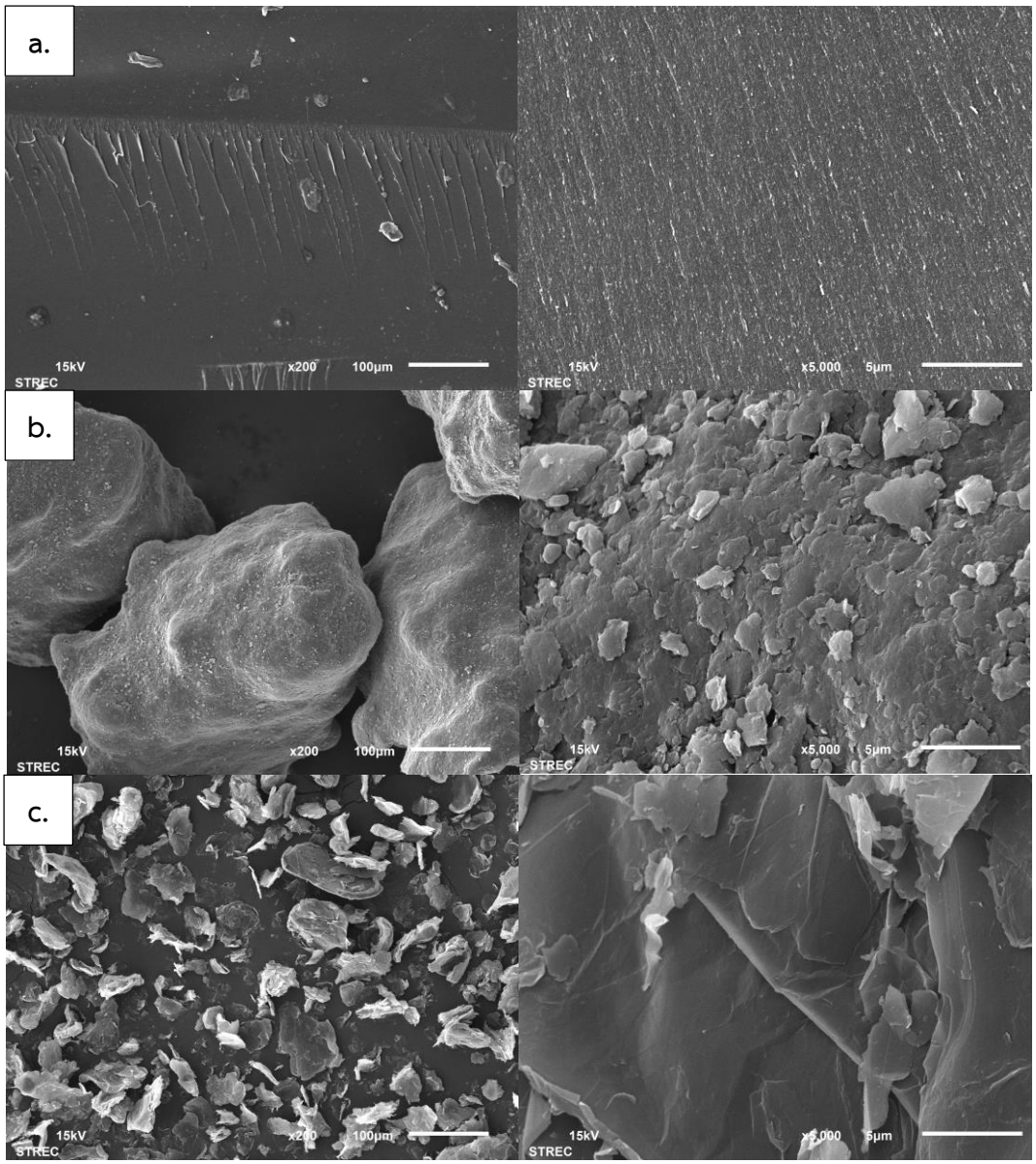

Figure 5.17 SEM micrographs of fracture surfaces of the polybenzoxazine composites:

a. neat polybenzoxazine

b. graphite

c. graphene

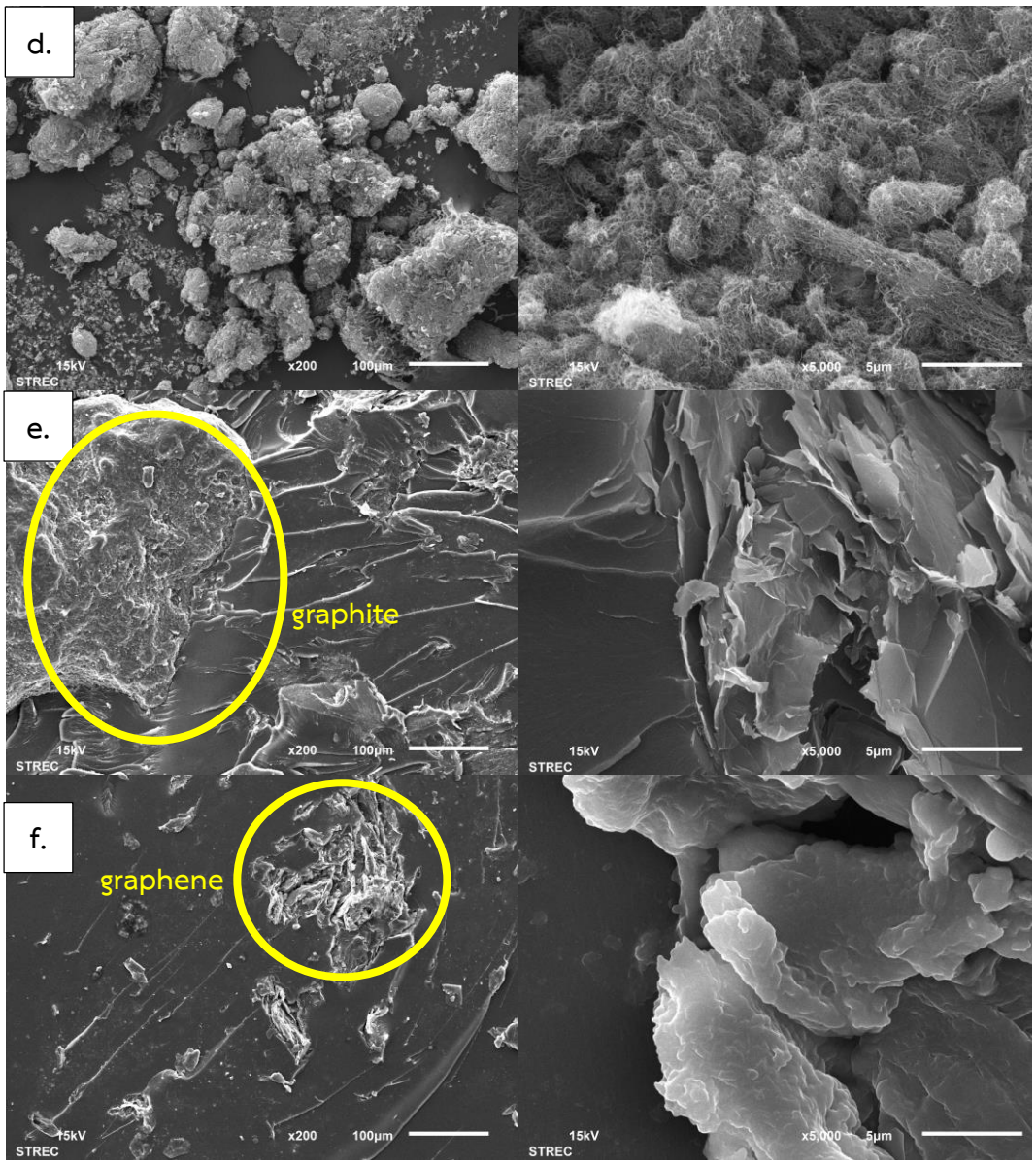

Figure 5.17 SEM micrographs of fracture surfaces of the polybenzoxazine composites:

d. carbon nanotubes

e. 0.5wt% graphite-filled polybenzoxazine composite

f. 0.5wt% graphene-filled polybenzoxazine composite

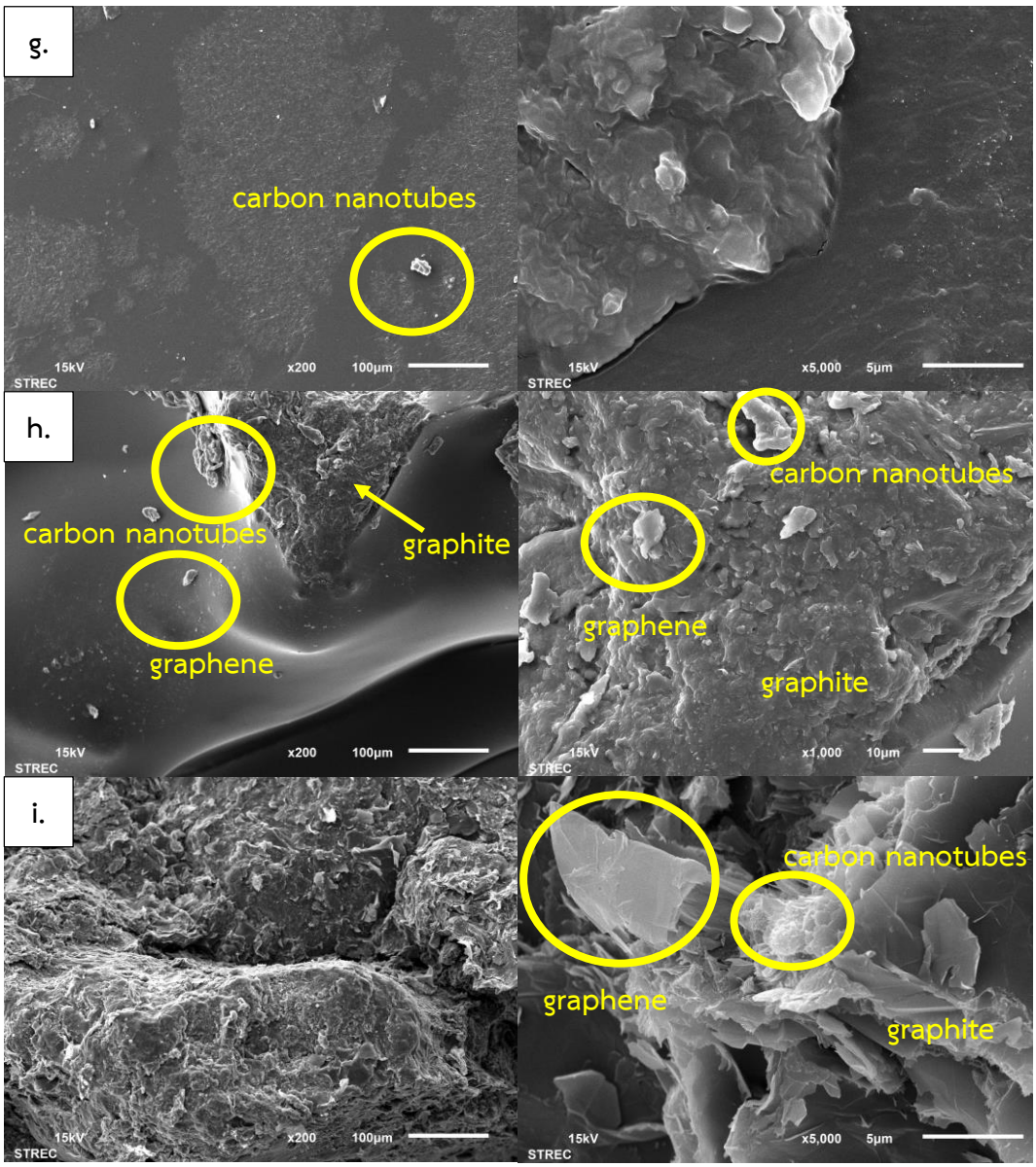

Figure 5.17 SEM micrographs of fracture surfaces of the polybenzoxazine composites:

g. 0.5wt% carbon nanotubes-filled polybenzoxazine composite

h. 0.5/0.5/0.5wt% graphite/graphene/carbon nanotubes-filled polybenzoxazine composite

i. 74.5/7.5/2wt% graphite/graphene/carbon nanotubes-filled polybenzoxazine composite

CHAPTER VI

CONCLUSIONS

The graphite/graphene/carbon nanotubes highly-filled polybenzoxazine composites were achieved in this research. The total content of fillers was constant at 84wt% where the content of carbon nanotubes were varied from 0-2 wt% at an expense of graphite. This appropriate content of fillers were confirmed by comparing their actual densities with theoretical densities.

The DSC thermograms implied that carbon nanotubes acted as a catalyst to accerelate ring opening polymerization of the oxazine ring. Carboxylic group were presented in these fillers confirmed by FTIR spectra. The DSC thermograms also revealed that the suitable condition to achieve fully-cured composites were 2 hours at temperature of 200°C and pressure of 15 MPa.

Such properties of the composite filled with carbon nanotubes were improved such as storage modulus, glass transition temperature, thermal degradation temperature, flexural properties, thermal and electrical conductivity. Carbon nanotubes which have tubular structure with long length and short diameter can randomly orient in the composite and attached with graphite and graphene efficiently resulting in great enhancement of thermal and electrical conductivity of the composite. Thermal conductivity of the composite filled with carbon nanotubes as

low as 0.5wt% was 21.3 W/m·K which achieved minimum requirements by the United States Department of Energy (DOE). In addition, electrical conductivity, flexural strength and modulus of the composite met those requirement by DOE as well.

Finally, polybenzoxazine composite filled with 76wt% graphite, 7.5wt% graphene, and 0.5wt% carbon nanotubes was proposed to be a good candidate to apply as bipolar plates in proton exchange membrane fuel cells because it provided the highest thermal conductivity and lowest water absorption where other relavant properities i.e. electrical conductivity, flexural strength, and flexural modulus were also achieved minimum requirements by the United States Department of Energy (DOE).

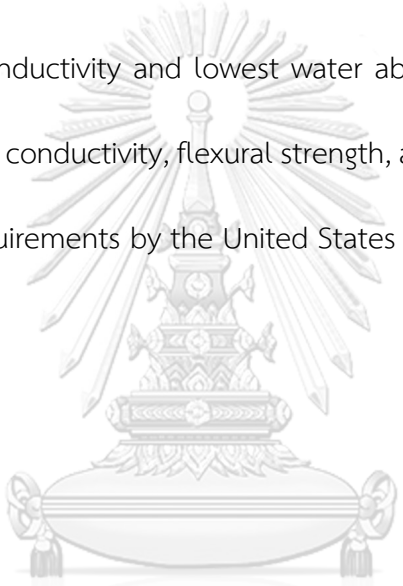

REFERENCES

[1] Electrographite Carbon Company Limited, *Carbon & Graphite Electrodes*. 2011 [cited 2016 Aug 2]; Available from: http://www.electrographite.co.za/products-materials/carbon-graphite-electrodes.

[2] Iwan, A., Malinowski, M., and Pasciak, G., Polymer fuel cell components modified by graphene: Electrodes, electrolytes and bipolar plates. Renewable and Sustainable Energy Reviews, 2015. 49: p. 954-967.

[3] Peighambardoust, S.J., Rowshanzamir, S., and Amjadi, M., Review of the proton exchange membranes for fuel cell applications. International Journal of Hydrogen Energy, 2010. 35(17): p. 9349-9384.

[4] Vishnyakov, V.M., Proton exchange membrane fuel cells. Vacuum, 2006. 80(10): p. 1053-1065.

[5] Zaratest, *Yakıt Hücreleri - (Pragma Industries) Hidrojen Enerjisi ve Yakıt Pili Deney Setleri - Mühendislik Deney Setleri*. 2008 [cited 2016 Aug 22]; Available from: http://www.zaratest.com.tr/curunler.php?kat=37.

[6] Kang, K., Park, S., and Ju, H., Effects of type of graphite conductive filler on the performance of a composite bipolar plate for fuel cells. Solid State Ionics, 2014. 262: p. 332-336.

[7] Plengudomkit, R., Okhawilai, M., and Rimdusit, S., Highly filled graphene-benzoxazine composites as bipolar plates in fuel cell applications. Polymer Composites, 2014: p. 1-13.

[8] Taherian, R., A review of composite and metallic bipolar plates in proton exchange membrane fuel cell: Materials, fabrication, and material selection. Journal of Power Sources, 2014. 265: p. 370-390.

[9] Du, L. and Jana, S.C., Hygrothermal effects on properties of highly conductive epoxy/graphite composites for applications as bipolar plates. Journal of Power Sources, 2008. 182(1): p. 223-229.

[10] Hermann, A., Chaudhuri, T., and Spagnol, P., Bipolar plates for PEM fuel cells: A review. International Journal of Hydrogen Energy, 2005. 30(12): p. 1297-1302.

[11] Hwang, I.U., Yu, H.N., Kim, S.S., Lee, D.G., Suh, J.D., Lee, S.H., Ahn, B.K., Kim, S.H., and Lim, T.W., Bipolar plate made of carbon fiber epoxy composite for polymer electrolyte membrane fuel cells. Journal of Power Sources, 2008. 184(1): p. 90-94.

[12] U.S.Department of Energy, *Technical Plan-Fuel Cells*. 2012 [cited 2016 May 13]; Available from: http://www1.eere.energy.gov/hydrogenandfuelcells/mypp/pdfs/fuel_cells.pdf.

[13] Yeetsorn, R., Fowler, M.W., and Tzoganakis, C., A Review of Thermoplastic Composites for Bipolar Plate Materials in PEM Fuel Cells, in Nanocomposites with Unique Properties and Applications in Medicine and Industry, J. Cuppoletti, Editor. 2011, InTech: Rijeka. p. 317.

[14] Yuan, W., Tang, Y., Yang, X., and Wan, Z., Porous metal materials for polymer electrolyte membrane fuel cells – A review. Applied Energy, 2012. 94: p. 309-329.

[15] Ishida, H., *Process for preparation of other publications benzoxazine compound in solventless system U.S. Patent 5,543,516*, 1996.

[16] Ishida, H. and Agag, T., Handbook of Benzoxazine. 2011, New York: Elsevier.

[17] Ishida, H. and Rimdusit, S., Very high thermal conductivity obtained by boron nitride-filled polybenzoxazine. Thermochimica Acta, 1998. 320: p. 177-186.

[18] Jubsilp, C., Punson, K., Takeichi, T., and Rimdusit, S., Curing kinetics of Benzoxazine–epoxy copolymer investigated by non-isothermal differential scanning calorimetry. Polymer Degradation and Stability, 2010. 95(6): p. 918-924.

[19] Kiskan, B., Ghosh, N.N., and Yagci, Y., Polybenzoxazine-based composites as high-performance materials. Polymer International, 2011. 60(2): p. 167-177.

[20] Zeng, M., Wang, J., Li, R., Liu, J., Chen, W., Xu, Q., and Gu, Y., The curing behavior and thermal property of graphene oxide/benzoxazine nanocomposites. Polymer, 2013. 54(12): p. 3107-3116.

[21] Dueramae, I., Pengdam, A., and Rimdusit, S., Highly filled graphite polybenzoxazine composites for an application as bipolar plates in fuel cells. Journal of Applied Polymer Science, 2013: p. 3909-3918.

[22] Dhakate, S., Mathur, R., Kakati, B., and Dhami, T., Properties of graphite-composite bipolar plate prepared by compression molding technique for PEM fuel cell. International Journal of Hydrogen Energy, 2007. 32(17): p. 4537-4543.

[23] Kimura, H., Ohtsuka, K., and Matsumoto, A., Performance of graphite filled composite based on benzoxazine resin. Journal of Applied Polymer Science, 2010. 117: p. 1711-1717.

[24] Adloo, A., Sadeghi, M., Masoomi, M., and Pazhooh, H.N., High performance polymeric bipolar plate based on polypropylene/graphite/graphene/nano-carbon black composites for PEM fuel cells. Renewable Energy, 2016. 99: p. 867-874.

[25] Dhakate, S.R., Sharma, S., Chauhan, N., Seth, R.K., and Mathur, R.B., CNTs nanostructuring effect on the properties of graphite composite bipolar plate. International Journal of Hydrogen Energy, 2010. 35(9): p. 4195-4200.

[26] Ghosh, A., Goswami, P., Mahanta, P., and Verma, A., Effect of carbon fiber length and graphene on carbon-polymer composite bipolar plate for PEMFC. Journal of Solid State Electrochemistry, 2014. 18(12): p. 3427-3436.

[27] Hsiao, M.-C., Liao, S.-H., Yen, M.-Y., Teng, C.-C., Lee, S.-H., Pu, N.-W., Wang, C.-A., Sung, Y., Ger, M.-D., Ma, C.-C.M., and Hsiao, M.-H., Preparation and properties of a graphene reinforced nanocomposite conducting plate. Journal of Materials Chemistry, 2010. 20(39): p. 8496.

[28] Kakati, B.K., Sathiyamoorthy, D., and Verma, A., Electrochemical and mechanical behavior of carbon composite bipolar plate for fuel cell. International Journal of Hydrogen Energy, 2010. 35(9): p. 4185-4194.

[29] Phuangngamphan, M., Development of Highly Thermally Conductive Graphite/ Graphene Filled Polybenzoxazine for Bipolar Plates in Fuel Cells. Master, Chemical Engineering, Chulalongkorn University, 2016.

[30] Laboratory of Advanced Energy Systems, *Fuel Cells Types*. 2007 [cited 2016 Aug 29]; Available from: http://tfy.tkk.fi/aes/AES/projects/renew/fuelcell/fc_2.html.

[31] Rosli, R.E., Sulong, A.B., Daud, W.R.W., Zulkifley, M.A., Husaini, T., Rosli, M.I., Majlan, E.H., and Haque, M.A., A review of high-temperature proton exchange

membrane fuel cell (HT-PEMFC) system. International Journal of Hydrogen Energy, 2016.

[32] Fuel Cell Today, *PEMFC*. 2016 [cited 2016 Aug 29]; Available from: http://www.fuelcelltoday.com/technologies/pemfc.

[33] Garche, J. and Dyer, C.K., Encyclopedia of Electrochemical Power Sources. Vol. 1. 2009, Spain: Elsevier.

[34] Tawfik, H., Hung, Y., and Mahajan, D., Metal bipolar plates for PEM fuel cell—A review. Journal of Power Sources, 2007. 163(2): p. 755-767.

[35] Dihrab, S.S., Sopian, K., Alghoul, M.A., and Sulaiman, M.Y., Review of the membrane and bipolar plates materials for conventional and unitized regenerative fuel cells. Renewable and Sustainable Energy Reviews, 2009. 13(6-7): p. 1663-1668.

[36] Wang, H. and Turner, J.A., Reviewing Metallic PEMFC Bipolar Plates. Fuel Cells, 2010. 10(4): p. 510-519.

[37] Ryan, C. *Green Machine Competition - Fuel Cell Pressurized Air Bipolar Plate (Cathode Side)*. 2007 [cited 2016 Aug 2]; Available from: https://www.chiefdelphi.com/media/photos/26116.

[38] Antunes, R.A., de Oliveira, M.C.L., Ett, G., and Ett, V., Carbon materials in composite bipolar plates for polymer electrolyte membrane fuel cells: A review of the main challenges to improve electrical performance. Journal of Power Sources, 2011. 196(6): p. 2945-2961.

[39] Koç, M. and Mahabunphachai, S., Feasibility investigations on a novel micro-manufacturing process for fabrication of fuel cell bipolar plates: Internal pressure-assisted embossing of micro-channels with in-die mechanical bonding. Journal of Power Sources, 2007. 172(2): p. 725-733.

[40] Kuilla, T., Bhadra, S., Yao, D., Kim, N.H., Bose, S., and Lee, J.H., Recent advances in graphene based polymer composites. Progress in Polymer Science, 2010. 35(11): p. 1350-1375.

[41] Pierson, H.O., Handbook of Carbon, Graphite, Diamond and Fullerene. 1993, Mill Road, Park Ridge, New Jersey: Noyes Publications.

[42] Toyo Tanso Company Limited, *Carbon-Graphite Products*. 2016 [cited 2017 Apr 25]; Available from: http://www.toyotanso.com/Products/Special_graphite/index.html.

[43] Wissler, M., Graphite and carbon powders for electrochemical applications. Journal of Power Sources, 2006. 156(2): p. 142-150.

[44] Hong, J., Park, D., W.,, and Shim, S., E., A Review on Thermal Conductivity of Polymer Composites Using Carbon-Based Fillers : Carbon Nanotubes and Carbon Fibers. Carbon Letters, 2010. 11: p. 347-356.

[45] Ferro-Ceramic Grinding Inc., *Graphite*. 2012 [cited 2016 Aug 22]; Available from: http://www.ferroceramic.com/graphite_table.htm.

[46] Geim, A.K., Novoselov, K.S., The Rise of Graphene. Nature Materials, 2007. 6: p. 183 - 191.

[47] Kim, H., Abdala, A.A., and Macosko, C.W., Graphene/Polymer Nanocomposites. Macromolecules, 2010. 43(16): p. 6515-6530.

[48] Shahil, K.M.F. and Balandin, A.A., Thermal properties of graphene and multilayer graphene: Applications in thermal interface materials. Solid State Communications, 2012. 152(15): p. 1331-1340.

[49] Goyal, V. and Balandin, A.A., Thermal properties of the hybrid graphene-metal nano-micro-composites: Applications in thermal interface materials. Applied Physics Letters, 2012. 100(7): p. 073113.

[50] Pradhan, N.R., Duan, H., Liang, J., and Iannachione, G.S., The specific heat and effective thermal conductivity of composites containing single-wall and multi-wall carbon nanotubes. Nanotechnology, 2009. 20: p. 1-7.

[51] Kaushik, B.K. and Kumar, M., Carbon Nanotubes: Properties and Applications, in Carbon Nanotube Based VLSI Interconnects: Analysis and Design, B.K. Kaushik and M.K. Majumder, Editors. 2015, Springer: New Delhi. p. 17-37.

[52] Ponnamma, D., Sadasivuni, K., K.,, Grohens, Y., Guo, Q., and Thomas, S., Carbon nanotube based elastomer composites – an approach towards multifunctional materials. Journal of Materials Chemistry C, 2014. 2: p. 8446-8485.

[53] Harris, P.J.F., Carbon Nanotubes and Related Structures: New Materials for the Twenty-first Century. 1999, United Kingdom: Cambridge University Press.

[54] Seetharamappa, J., Yellappa, S., and D'Souza, F., Carbon Nanotubes: Next Generation of Electronic Materials. The Electrochemical Society Interface, 2006. 15(2): p. 23-25,61.

[55] Weisman R. Bruce and Shekhar, S., Carbon Nanotubes. The Electrochemical Society Interface, 2006. 15(2): p. 42-46.

[56] Karachevtsev, V.A., Nanobiophysics: Fundamentals and Applications. 2016, Singapore: Pan Stanford Publishing.

[57] Planes, E., Flandin, L., and Alberola, N., Polymer Composites Bipolar Plates for PEMFCs. Energy Procedia, 2012. 20: p. 311-323.

[58] Tanaka, K. and Iijima, S., Carbon Nanotubes and Graphene. 2 ed. 2014, Massachusetts: Elsevier.

[59] Rimdusit, S., Tiptipakorn, S., Jubsilp, C., and Takeichi, T., Polybenzoxazine alloys and blends: Some unique properties and applications. Reactive and Functional Polymers, 2013. 73(2): p. 369-380.

[60] Rimdusit, S., Jubsilp, C., and Tiptipakorn, S., Alloys and Composites of Polybenzoxazines Properties and Application. 2013, Singapore: Springer.

[61] Nair, C., Advances in addition-cure phenolic resins. Progress in Polymer Science, 2004. 29(5): p. 401-498.

[62] Tian, X., Itkis, M.E., Bekyarova, E.B., and Haddon, R.C., Anisotropic Thermal and Electrical Properties of Thin Thermal Interface Layers of Graphite Nanoplatelet-Based Composites. Scientific Reports, 2013. 3.

[63] Rimdusit, S. and Ishida, H., Development of new class of electronic packaging materials based on ternary systems of benzoxazine, epoxy, and phenolic resins. Polymer, 2000. 41: p. 7941-7949.

[64] Yu, A., Ramesh, P., Sun, X., Bekyarova, E., Itkis, M.E., and Haddon, R.C., Enhanced Thermal Conductivity in a Hybrid Graphite Nanoplatelet - Carbon Nanotube Filler for Epoxy Composites. Advanced Materials, 2008. 20(24): p. 4740-4744.

[65] Lu, T., Ye, H., Zheng, A., Xu, X., Xu, C., Wang, H., Sun, L., and Xu, L., Hybrid modification of high-density polyethylene with hyperbranched polyethylene-functionalized multiwalled carbon nanotubes and few-layered graphene. Journal of Applied Polymer Science, 2017. 134(27): p. 44848.

[66] Che, J., Wu, K., Lin, Y., Wang, K., and Fu, Q., Largely improved thermal conductivity of HDPE/expanded graphite/carbon nanotubes ternary composites via filler network-network synergy. Composites Part A: Applied Science and Manufacturing, 2017. 99: p. 32-40.

[67] Zakaria, M.R., Kudus, M.H.A., Md. Akil, H., and Mohd, M.Z.T., Comparative study of graphene nanoparticle and multiwall carbon nanotube filled epoxy nanocomposites based on mechanical, thermal and dielectric properties. Composites Part B: Engineering, 2017. 119: p. 57-66.

[68] XG Sciences, *XGnP® Graphene Nanoplatelets: Grade H*. 2017; Available from: http://xgsciences.com/products/graphene-nanoplatelets/grade-h/.

[69] Nano Generation Company Limited, *Multi-walled Carbon Nanotubes*. 2017 [cited 2017 Jun 26]; Available from: http://www.nanogenstore.com/index.php?route=product/product&path=63&product_id=191.

[70] Smits, F.M., Measurement of Sheet Resistivities with the Four-Point Probe. The Bell System Technical Journal 1958. 37: p. 711-718.

[71] Senna, J.R. *Finite-Size Corrections for 4-Point Probe Measurements* 2004 [cited 2017 Oct 12]; Available from: http://four-point-probes.com/finite-size-corrections-for-4-point-probe-measurements/.

[72] Pandey, A.K., Singh, K., and Kar, K.K., Thermo-mechanical properties of graphite-reinforced high-density polyethylene composites and its structure–property corelationship. Journal of Composite Materials, 2016. 51(12): p. 1769-1782.

[73] German, R.M., Particle Packing Characteristics, Metel Powder Industries Federation. 1989: Princeton.

[74] Kasemsiri, P., Hiziroglu, S., and Rimdusit, S., Effect of cashew nut shell liquid on gelation, cure kinetics, and thermomechanical properties of benzoxazine resin. Thermochimica Acta, 2011. 520: p. 84-92.

[75] Phuangngamphan, M. and Rimdusit, S. Effect of graphite aggregate sizes on thermal and mechanical properties of graphite/benzoxazine composite bipolar plate for polymer electrolyte membrane fuel cell in Pure and Applied Chemistry International Conference. 2016. BITEC, Bangkok, Thailand.

[76] Jubsilp, C., Singto, J., Yamo, W., and Rimdusit, S., Effect of Graphite Particle Size on Tribological and Mechanical Properties of Polybenzoxazine Composites. Chemical Engineering Transactions, 2017. 57.

[77] Corcione, C. and Frigione, M., Characterization of Nanocomposites by Thermal Analysis. Materials, 2012. 5(12): p. 2960-2980.

[78] Witpathomwong, S. and Rimdusit, S. Effects of carbon nanotube contents on viscoelastic properties and thermal stability of polybenzoxazine composites in Pure and Applied Chemistry International Conference. 2017. Centra Government Complex Hotel & Convention Centre, Bangkok, Thailand

[79] Ishida, H. and Rimdusit, S., Heat Capacity Measurement of Boron Nitride-filled Polybenzoxazine: The composite structure-insensitive property. Journal of Thermal Analysis and Calorimetry, 1999. 58(3): p. 497-507.

[80] Berman, R., Thermal Conduction in Solids. 1976, Oxford: Clarendon Press.

[81] Tritt, T., M., Thermal Conductivity: Theory, Properties, and Applications. 2004, South Carolina: Plenum.

[82] Rungsima, Y., Development of Electrically Conductive Thermoplastic Composites for Bipolar Plate Application in Polymer Electrolyte Membrane Fuel Cell. Doctor Chemical Engineering, Waterloo, 2010.

[83] Kara, S., Arda, E., Dolastir, F., and Pekcan, O., Electrical and optical percolations of polystyrene latex-multiwalled carbon nanotube composites. J Colloid Interface Sci, 2010. 344(2): p. 395-401.

[84] Du, J., Zhao, L., Zeng, Y., Zhang, L., Li, F., Liu, P., and Liu, C., Comparison of electrical properties between multi-walled carbon nanotube and graphene nanosheet/high density polyethylene composites with a segregated network structure. Carbon, 2011. 49(4): p. 1094-1100.

[85] Dumas, L., Bonnaud, L., and Dubois, P., Polybenzoxazine Nanocomposites: Case Study of Carbon Nanotubes, in Advanced and Emerging Polybenzoxazine Science and Technology, H. Ishida and P. Froimowicz, Editors. 2017, Elsevier: Amsterdam. p. 767-800.

[86] Zulfli, N.H.M., Bakar, A.A., and Chow, W.S., Mechanical and water absorption behaviors of carbon nanotube reinforced epoxy/glass fiber laminates. Journal of Reinforced Plastics and Composites, 2013. 32(22): p. 1715-1721.

APPENDICES

APPENDICES

Appendix A Size distribution of graphite, graphene, and carbon nanotubes

Appendix A-1 Size distribution of graphite.

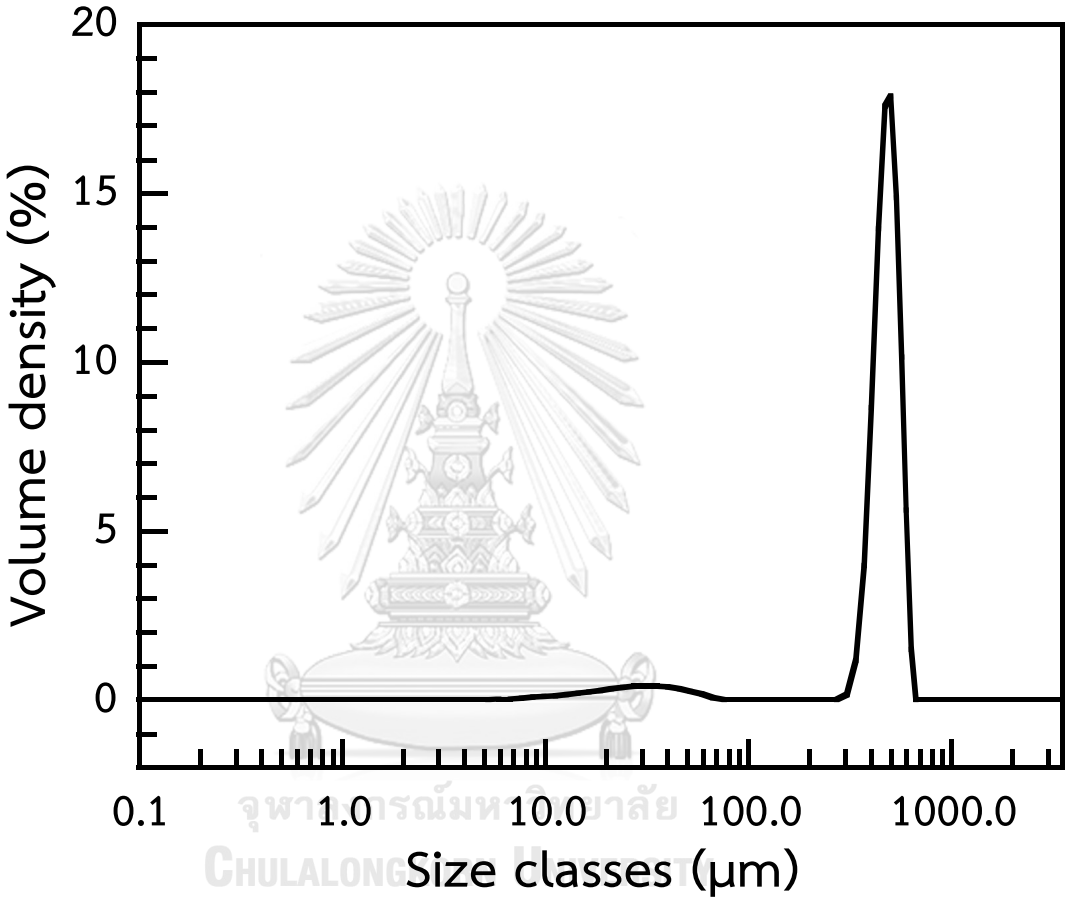

Appendix A-2 Size distribution of graphene.

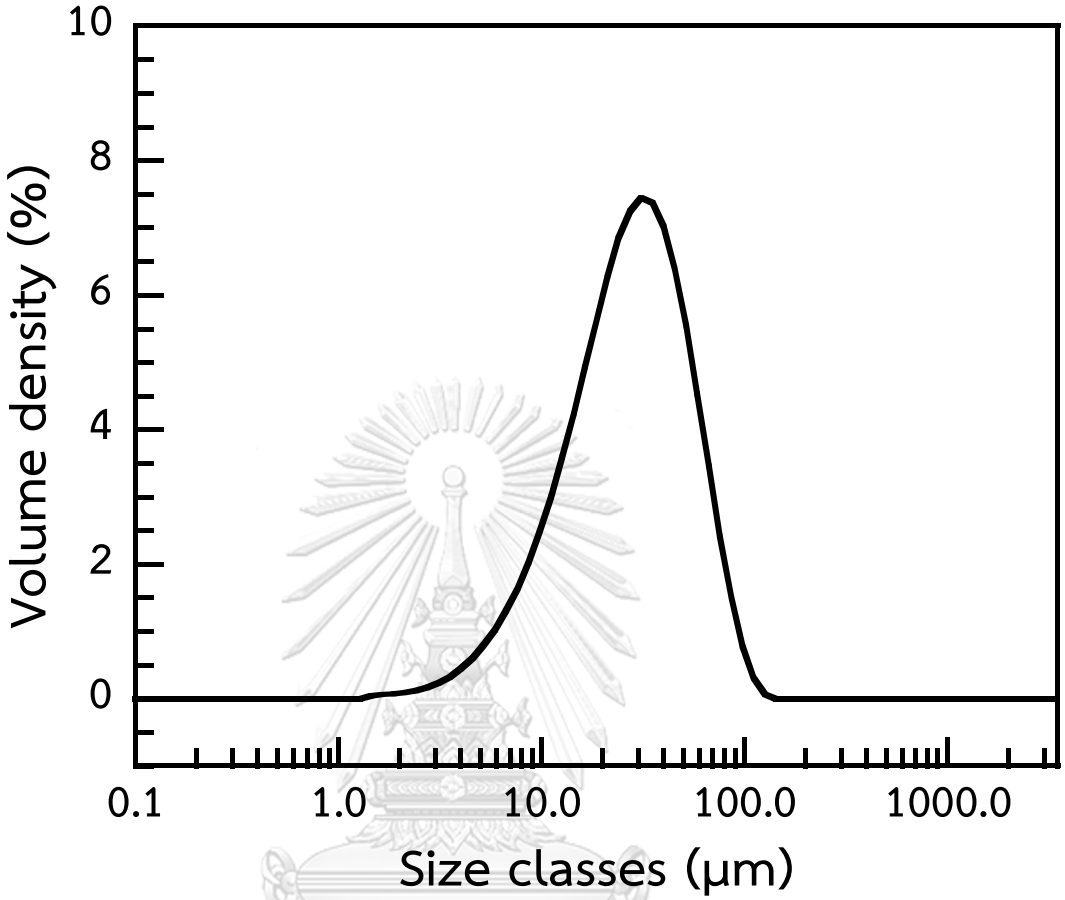

Appendix A-3 Size distribution of carbon nanotubes.

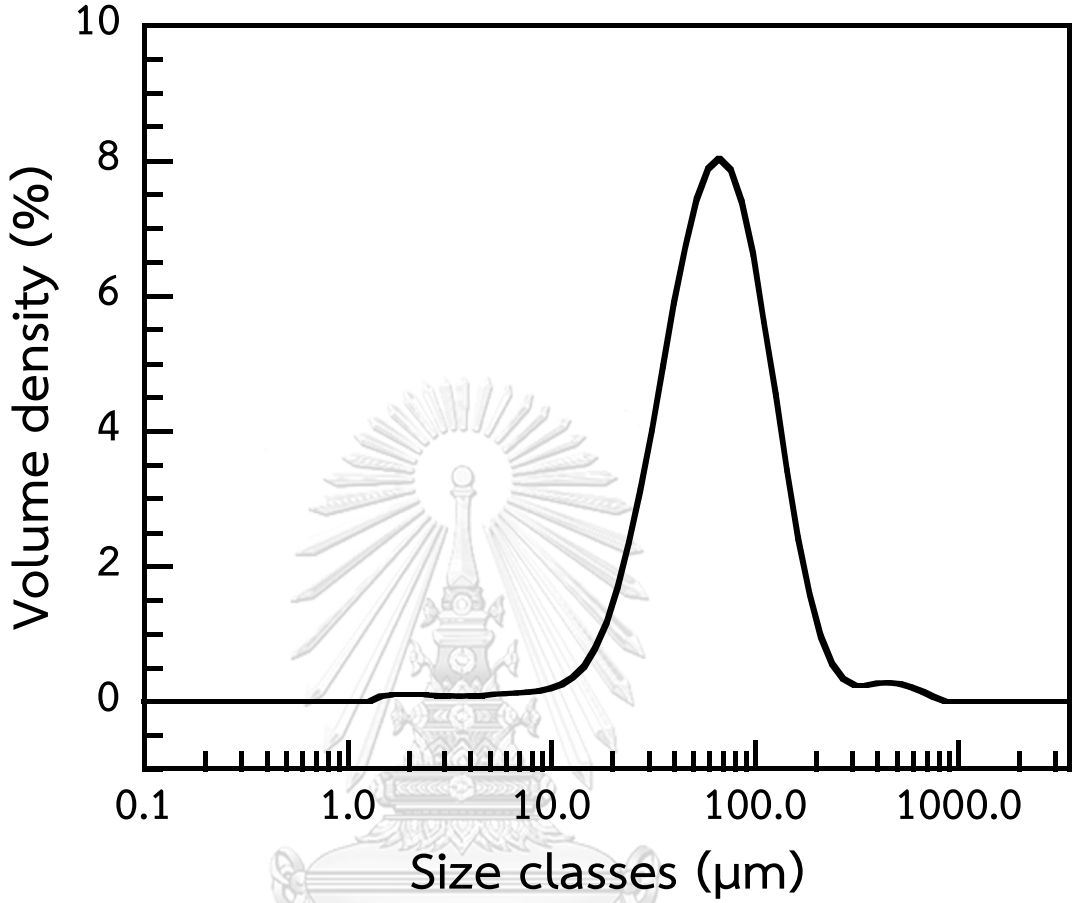

Appendix B Characterizaion of graphite/graphene/carbon nanotubes filled polybenzoxazine composite.

Appendix B-1 Theoretical density and actual density of graphite/graphene/carbon nanotubes filled polybenzoxazine composite.

Fillers content (wt%)			Density (g/cm^3)	
Graphite	Graphene	Carbon nanotubes	Theoretical	Actual
0.0	0.0	0.0	1.190	-
70.0	0.0	0.0	1.661	1.670
75.0	0.0	0.0	1.709	1.705
80.0	0.0	0.0	1.760	1.758
83.0	0.0	0.0	1.793	1.790
84.0	0.0	0.0	1.804	1.802
85.0	0.0	0.0	1.815	1.804
76.5	7.5	0.0	1.815	1.825
76.0	7.5	0.5	1.815	1.821
75.5	7.5	1.0	1.815	1.812
75.0	7.5	1.5	1.815	1.814
74.5	7.5	2.0	1.815	1.815

Appendix B-2 Storage moduli (E') at 25°C and glass transition temperatures (T_g) which obtained from loss moduli of graphite/graphene/carbon nanotubes filled polybenzoxazine composite.

Filler content (wt%)			**E' (GPa)**	**T_g (°C)**
Graphite	**Graphene**	**Carbon nanotubes**		
0.0	0.0	0.0	5.2	171
76.5	7.5	0.0	9.6	198
76.0	7.5	0.5	9.7	201
75.5	7.5	1.0	10.0	203
75.0	7.5	1.5	10.3	203
74.5	7.5	2.0	11.4	207

Appendix B-3 Thermal degradation temperature at 5% weight loss (T_{d5}) and char yield at 800°C of graphite/graphene/carbon nanotubes filled polybenzoxazine composite.

Filler content (wt%)			T_{d5} (°C)	Char yield (%)	
Graphite	Graphene	Carbon nanotubes		Experimental	Theoretical
0.0	0.0	0.0	334	26.0	
76.5	7.5	0.0	422	93.3	87.39
76.0	7.5	0.5	423	90.9	87.37
75.5	7.5	1.0	428	90.6	87.35
75.0	7.5	1.5	442	90.2	87.34
74.5	7.5	2.0	466	89.9	87.32
100.0	0.0	0.0	>850	100.0	-
0.0	100.0	0.0	386	89.7	-
0.0	0.0	100.0	>850	96.8	-

Appendix B-4 Electrical conductivity of graphite/graphene/carbon nanotubes filled polybenzoxazine composite.

Filler content (wt%)			Electrical conductivity (S/cm)
Graphite	Graphene	Carbon nanotubes	
76.5	7.5	0.0	320 ± 3
76.0	7.5	0.5	333 ± 3
75.5	7.5	1.0	340 ± 6
75.0	7.5	1.5	360 ± 4
74.5	7.5	2.0	364 ± 4

Appendix B-5 Flexural properties of graphite/graphene/carbon nanotubes filled polybenzoxazine composite.

Filler content (wt%)			Flexural strength (MPa)	Flexural modulus (GPa)
Graphite	Graphene	Carbon nanotubes		
0.0	0.0	0.0	120.2 ± 5.2	5.5 ± 0.7
76.5	7.5	0.0	28.1 ± 0.5	20.9 ± 0.3
76.0	7.5	0.5	34.2 ± 4.2	36.5 ± 6.3
75.5	7.5	1.0	33.7 ± 3.8	34.8 ± 0.9
75.0	7.5	1.5	39.4 ± 3.2	37.7 ± 2.2
74.5	7.5	2.0	41.5 ± 2.9	49.7 ± 1.7

Appendix B-6 Water absorption of graphite/graphene/carbon nanotubes filled polybenzoxazine composite.

Filler content (wt%)			24 hours (%)	7 days (%)
Graphite	Graphene	Carbon nanotubes		
0.0	0.0	0.0	0.149 ± 0.022	0.387 ± 0.038
76.5	7.5	0.0	0.023 ± 0.021	0.037 ± 0.007
76.0	7.5	0.5	0.060 ± 0.010	0.104 ± 0.010
75.5	7.5	1.0	0.047 ± 0.006	0.118 ± 0.003
75.0	7.5	1.5	0.111 ± 0.047	0.201 ± 0.032
74.5	7.5	2.0	0.114 ± 0.046	0.230 ± 0.012

VITA

Mr. Sirawit Witpathomwong was born in Bangkok, Thailand on November 26, 1992. He graduated high school level in 2011 from Suankularb Wittayalai School. He received Bachelor's Degree of Chemical Engineering from Faculty of Engineering, Chulalongkorn University in 2015. After graduation, he continued his study for a Master's Degree of Chemical Engineering, Faculty of Engineering, Chulalongkorn University.

Some parts of this work were selected for oral presentations in the Pure and Applied Chemistry International Conference (PACCON) which was held during February 2-3, 2017 at Centra Government Complex Hotel and Convention Centre, Bangkok, Thailand and The International Thai Institute of Chemical Engineering and Applied Chemistry Conference (ITIChE) which was held during October 18-20, 2017 at Shangri-La Hotel, Bangkok, Thailand.